

# *Studies in Radar*

## *Cross-Sections-IV*

*Comparison Between Theory  
and Experiment of the  
Cross-Section of a Cone*

*by K. M. Siegel, H. A. Alperin,  
J. W. Crispin, H. E. Hunter, R. E. Kleinman,  
W. C. Orthwein, and C. E. Schensted*

*Project MIRO*  
*Contract No. AF 30(602)-9*

Expenditure Order Numbers:

RDO 166-17 R161-43

RDO 166-17 AD-4

RDO 166-17 AD-7

The research reported in this document has been made possible through support and sponsorship extended by The Rome Air Development Center under Contract No. AF 30(602)-9. It is published for technical information only and does not represent recommendations or conclusions of the sponsoring agency.

*Willow Run Research Center*  
*Engineering Research Institute*  
*University of Michigan*  
*UMM-92 February, 1953*

STUDIES IN RADAR CROSS-SECTIONS

- I "Scattering by a Prolate Spheroid" by F. V. Schultz.
- II "The Zeros of the Associated Legendre Functions  $P_n^m(\mu')$  of Non-Integral Degree" by K. M. Siegel, D. M. Brown, H. E. Hunter, H. A. Alperin, and C. W. Quillen.
- III "Scattering by a Cone" by K. M. Siegel and H. A. Alperin.
- IV "Comparison Between Theory and Experiment of the Cross-Section of a Cone" by K. M. Siegel, H. A. Alperin, J. W. Crispin, H. E. Hunter, R. E. Kleinman, W. C. Orthwein, and C. E. Schensted.<sup>1</sup>

<sup>1</sup> - Portions of this report were presented in a paper, "Scattering by a Semi-Infinite Cone" by K. M. Siegel and H. A. Alperin at the meeting of the American Physical Society held in Washington, D. C., on May 3, 1952.

TABLE OF CONTENTS

<u>Section :</u>	<u>Title</u>	<u>Page</u>
	List of Figures	ii
	List of Charts	ii
	List of Tables	ii
	Nomenclature	iii
	Preface	v
I	Introduction	1
II	Comparison Between Scalar Theory and Electromagnetic Theory	5
III	Special Summation Techniques	8
IV	The Wedge	11
V	The Cone	14
	A The Analytic Expressions for $\sigma$	14
	B $\sigma$ for Small Cone Angles	26
	C $\sigma$ for Other Cone Angles	32
VI	Conclusion	38
Appendix A	- The Determination of the Quantities $n_i$ , $m_i$ , $B_{n_i}$ , and $B_{m_i}$	41
Appendix B	- Certain Values of $n_i$ and $B_{n_i}$ Computed by the I. N. A.	57
Appendix C	- Derivation of Scalar and Vector Cross-Sections in the Large Cone Angle Case	58
Appendix D	- Derivation of an Integral Expression for the Sum Occurring in $\sigma'(0)$	61
Appendix E	- List of Errors Observed in UMM-87	66
	References	67
	Distribution	70

UMM-92

LIST OF FIGURES

<u>Number</u>	<u>Title</u>	<u>Page</u>
V-1	Geometry of Scattering from an Infinite Cone	21
V-2	Comparison between $\sigma'(0)$ , $\sigma(0)$ , $\sigma_{p.o.}(0)$ for the "Small Cone Angle" Approximations	33
V-3	Comparison between $\sigma'(0)$ , $\sigma(0)$ , and $\sigma_{p.o.}(0)$ for the "Large Cone Angle" Approximations	37
VI-1	Comparison between Theory and Experiment	39

LIST OF CHARTS

<u>Number</u>	<u>Title</u>	<u>Page</u>
A-I	Graph Representing "Best Values" of $\int_{x_0}^1 [P_{n_i}(x)]^2 dx$ vs. $n_i$ as Originally Computed	54
A-II	Graph Representing "Best Values" of $\frac{1}{m_i(m_i+1)}$ $\int_{x_0}^1 [P_{m_i}^1(x)]^2 dx$ vs. $m_i$ as Originally Computed	55
A-III	Graph Representing "Best Values" of $\int_{x_0}^1 [P_{n_i}(x)]^2 dx$ and $\frac{1}{m_i(m_i+1)} \int_{x_0}^1 [P_{m_i}^1(x)]^2 dx$	56

LIST OF TABLES

<u>Number</u>	<u>Title</u>	<u>Page</u>
A-1	Legendre Polynomials	47
A-1a	Derivatives (with respect to x) of the Legendre Polynomials	49
A-2	Values of Legendre Functions and Derivatives for $x = \cos 165^\circ$ and $y = i$	52
A-3	Values of $\int_{x_0}^1 [P_{n_i}(x)]^2 dx$ and $\int_{x_0}^1 [P_{m_i}^1(x)]^2 dx$ , $x_0 = \cos 165^\circ$	53

NOMENCLATURE

- $\vec{E}$  = electric field vector
- $k$  =  $2\pi/\lambda$
- $\lambda$  = wavelength
- $\sigma$  = the radar cross-section
- $\sigma_D$  = the differential scattering cross-section ( $\sigma = 4\pi \sigma_D$ )
- $j$  =  $\sqrt{-1}$
- $J_x(kr)$  = cylindrical Bessel function of degree  $x$  and argument  $kr$   
(in this report  $x$  almost always has the value  $n_i + 1/2$ )
- $P_n^m(\mu)$  = associated Legendre function of the first kind, order  $m$ ,  
degree  $n$ , and argument  $\mu$
- $n_i$  = real number defined by  $P_{n_i}^1(\mu_0) = 0$ , ( $n_i > -1/2$ )
- $m_i$  = real number defined by  $\left. \frac{dP_{m_i}^1(\mu)}{d\mu} \right|_{\mu = \mu_0} = 0$ , ( $m_i > -1/2$ )
- $r$  = distance from scatterer to field point in space
- $\mu$  =  $\cos \theta$  ( $\mu_0 = \cos \theta_0$ )
- $\theta_0$  = the supplement of  $1/2$  the total included cone angle  
(spherical coordinates)
- $\theta_1$  =  $\pi - \theta_0 = 1/2$  the total included cone angle
- $\theta_2$  =  $1/2$  the wedge angle
- $\sigma_{p.o.}(0)$  = the value of  $\sigma$  determined by physical optics

NOMENCLATURE (Continued)

$\sigma(0)$  = the value of  $\sigma$  determined by scalar theory

$\sigma'(0)$  = the value of  $\sigma$  determined by the exact methods of electromagnetic theory

$e^{-j\omega t}$  = the type of time dependence used throughout this paper with the exception of the discussion of the scalar case in Section V-A where  $e^{j\omega t}$  is used

$$\frac{\partial f(\mathbf{x}_0)}{\partial \mathbf{x}} = \left. \frac{\partial f(\mathbf{x})}{\partial \mathbf{x}} \right|_{\mathbf{x} = \mathbf{x}_0}$$

$z_x(kr)$  = the spherical Bessel function of order  $x$  and argument  $kr$

$\vec{A}(\vec{r})$  = the vector potential

$$B_{n_i} = \int_{\mu_0}^1 \left[ P_{n_i}^1(\mu) \right]^2 d\mu$$

$$B_{m_i} = \int_{\mu_0}^1 \left[ P_{m_i}^1(\mu) \right]^2 d\mu$$

$$\delta = \frac{1 - \cos \theta_1}{2}$$

$$\psi(x) = \frac{d}{dx} \left\{ \ln [\Gamma(x+1)] \right\}$$

$$o(\delta^2) : \lim_{\delta \rightarrow 0} \frac{o(\delta^2)}{\delta^2} = 0$$

$$O(\delta^2) : \lim_{\delta \rightarrow 0} \frac{O(\delta^2)}{\delta^2} = \text{constant} \neq 0 \text{ or } \infty.$$

PREFACE

This paper has one central purpose, the determination by exact electromagnetic theory of the radar cross-section of a semi-infinite cone. The result obtained is compared with experiment and with the cross-sections obtained by the approximate methods of physical optics and scalar theory.

Part I contains an explanation of why there is an interest in the problem and a review of some of the historical background.

Part II contains a discussion of the reasoning which leads one to consider scalar approximations.

Part III contains a discussion of the role that special summation techniques can have in research dealing with scattering problems. It is shown why these summation techniques can become a valuable aid in such research and how, a priori, one may state whether summation techniques should be used.

In Part IV the fact that summation techniques had really been used previously in scattering problems is exhibited. The wedge is used as an example.

The radar cross-section of a semi-infinite cone is discussed in Part V, and the results of the theoretical evaluations are compared with experiment in the Conclusion.

The Appendices are self-explanatory when associated with those portions of the text where they are referenced.

This paper is the fourth in a series of reports dealing with the problems of the scattering of microwaves by various bodies. The third in this series contained a review of the work previously done on the cone problem and the beginnings of the analysis leading up to the work reported in this paper. This paper completes the consideration of the problem of determining the radar cross-section of a semi-infinite cone for the case of axially-symmetric back-scattering.





## I

INTRODUCTION

In order to determine the radar cross-section of an object of specified shape and size, it is necessary to solve a vector equation,  $(\nabla^2 + k^2) \vec{E} = 0$ , subject to vector boundary conditions. This equation was first stated in the 19th century by Helmholtz, and the complete solution was obtained about 50 years ago by Mie for a sphere. Since that time complete solutions have been obtained for a small number of other bodies. The results obtained from the solution of this equation for one additional body, the semi-infinite cone, are discussed in this paper.

SEMI-INFINITE CONE

Since all real objects are finite in size, it becomes necessary (from a practical point of view) to justify the effort involved in obtaining a solution for the semi-infinite cone. The justification is that the solution of the semi-infinite cone problem leads directly to the solutions for many shapes of practical interest. These shapes include almost all pointed bodies of revolution and many actual missile shapes.

One reason for approaching the problem of the semi-infinite cone before approaching the problem of the finite cone is because the problem is easier to solve. This follows since it is possible to express the semi-infinite conic surface as a contour surface ( $\theta = \text{constant}$ ) in spherical coordinates.

Furthermore, the cross-section of the semi-infinite cone remains unchanged in many cases when the sides of the cone are curved back and smoothly terminated. Thus, for example, it can be shown that the cross-section of an ogive (the minor segment of a circle revolved around its chord) is approximately equal to the cross-section of a semi-infinite cone having the same angle at the

nose, if the radar is on or near the axis of the cone or ogive.<sup>1</sup> The ogive is an extremely important missile nose configuration.

The cross-section of a finite cone and of many actual missile shapes which are not easily represented by any simple geometric figures can also be approximated in many cases by the cross-section of a semi-infinite cone. The cross-section of the semi-infinite cone is due essentially to tip-scattering, as is shown in this paper. Similarly, the cross-section of the ogive, if viewed from near the axis is also due to tip-scattering. Finally, the cross-section of a finite cone if viewed from nose-on or near nose-on is due to contributions from the tip and the base. However, if the base is rough, the phases of the waves scattered from the base will generally be such as to cancel one another almost completely so that once again the principal contribution is from the tip. As a first approximation many missiles, when viewed from nose-on or near nose-on, may be so considered.

#### METHODS OF SOLUTION

The determination of the exact solution of the vector Helmholtz equation is an extremely difficult task. A number of approximations to this solution are possible in specific cases. When the wavelength is large with respect to the characteristic dimension of the scatterer, the Rayleigh approximation is valid. If the wavelength is small with respect to the characteristic dimension of the scatterer, the methods of physical optics are applicable. In the limit of vanishing wavelength the simple methods of geometric optics are applicable. The sound theory solution, in which a scalar equation is substituted for the vector equation, is often very useful. The application of these considerations to the case of the semi-infinite cone is puzzling, since the characteristic dimension which can be associated with the object is infinite. This would lead one to guess that the wavelength is always small with respect to the characteristic dimension, and that the physical optics approximation is quite accurate for all finite wavelengths. This indeed

---

<sup>1</sup>Providing the wavelength is very much smaller than the maximum diameter of the ogive.

turns out to be the case. In this paper it is shown that a physical optics approximation computed by the current distribution method is virtually identical with the exact value of cross-section obtained from the vector equation. In fact, the agreement between these two determinations of  $\sigma$  is better than the agreement between the exact solution and the best experimental measurements, although the agreement between theory and experiment is quite good. In addition, it might appear at first glance that geometric optics would be applicable. However, since the principal cross-section contribution is due to scattering from the tip, geometric optics yields no information because it predicts a cross-section of zero.

### TYPES OF SOLUTIONS

A complete solution to the problem of the semi-infinite cone would involve first, the case in which the transmitter and the receiver are coincident and on the axis of the cone; second, an extension to those values of  $\sigma$ , where the receiver and transmitter are coincident but off the axis of the cone; and third, an extension to values of  $\sigma$ , where the receiver and transmitter are separated. The equations derived in this paper suffice for the solutions of the first case and numerical results have been computed only for that case. Extension to the second and third cases would require modifications of the mathematical methods.

### OTHER WORK ON THIS PROBLEM

This paper is the fourth in a series designed with the ultimate purpose of presenting sufficient cross-section material of a general nature to allow one to predict missile cross-sections to within the accuracy required by defensive missile system designers. Hence, the cone is presented as one facet of the whole problem. In addition, certain allied topics stemming from the third in this series of cross-section studies are presented. For this reason UMM-87, "Studies in Radar Cross-Sections - III, Scattering by a Cone", should be read prior to this paper. In particular, careful observation should be made (in UMM-87) of the mathematical relations

that exist between the scalar and vector cone solutions.<sup>1</sup> A fuller understanding of the significance of scalar solutions appears to be necessary. Consequently, a portion of this paper is used to discuss the meaning of the scalar solution and/or the sound solution as applied to the vector problem. This discussion is by no means exhaustive, and it is hoped that it will serve as a stimulus for further research.

The Hansen and Schiff wedge solution is also discussed because it allows one to think in terms of trigonometric functions and clearly points out the type of difficulties one must overcome in the cone problem.

This paper makes extensive use of the works of Spencer (Ref. 1), Hansen (Ref. 2), Hansen and Schiff (Ref. 3, 4, and 5) and Sletten (Ref. 6). Without their individual work, whole sections of this report would not appear. If their collective work had not appeared, the basis of this report would not exist.

---

<sup>1</sup>Since the reader has been referred to UMM-87, it should be pointed out that Appendix E of this report contains corrections to errors in UMM-87.

## II

COMPARISON BETWEEN SCALAR THEORY  
AND ELECTROMAGNETIC THEORY

The steady state scattering of a harmonic electromagnetic wave may be expressed in terms of the solution of the vector Helmholtz equation,  $(\nabla^2 + k^2) \vec{E} = 0$ , subject to vector boundary conditions. If a plane wave is incident on the scattering body, then the differential scattering cross-section is defined by

$$\sigma_D = \lim_{r \rightarrow \infty} r^{n-1} \left| \frac{\vec{E}_S}{\vec{E}_I} \right|^2$$

where  $\vec{E}_S$  is the scattered field,

$\vec{E}_I$  is the incident field,

$r$  is the distance between the scatterer and the point at which  $\vec{E}_S$  is measured, and

$n$  is the number of dimensions of the space.

Since a scalar equation is usually easier to solve than a vector equation, it is of interest to determine the circumstances under which an electromagnetic cross-section can be approximated by some appropriate scalar cross-section.

This problem has already been considered in some detail by R. C. Spencer (Ref. 1). He states that under certain assumptions "P. M. Austin (Ref. 7) has shown that, for the special case of back-scattering, electromagnetic theory leads to the same results that would have been obtained by the simpler scalar theory of sound and physical optics. Moreover, [it is also shown that under the same assumptions] the polarization of the back-scattered radiation coincides with the incident polarization."

The assumptions (or simplifications to the electromagnetic theory) mentioned above are, as listed by Spencer:

1. the incident wave is plane;
2. the surface is perfectly conducting; and
3. the current distribution over the illuminated region of the surface is obtained on the assumption that at every point the incident field is reflected as though an infinite plane wave were incident on the infinite tangent plane.

Whenever the radii of curvature of the scattering body are at every point large compared with the wavelength, the third assumption would appear to be a valid simplification of the electromagnetic problem. Furthermore, a "ray" treatment of the problem would be expected to produce the same results for either a vector or scalar problem in the limit of vanishing wavelength. Thus, Austin's conclusion that the cross-section of a smooth body obtained from scalar sound theory will agree with the cross-section obtained from electromagnetic theory (at least for back-scattering) is verified whenever the incident wavelength is sufficiently small.

If the ratio,  $\lambda/\rho$  is very large,<sup>1</sup> the Rayleigh scattering law applies and the cross-sections for sound and electromagnetic waves have the same dependence on wavelength. Thus, these cross-sections agree with one another to within a constant factor. For example, the back-scattering cross-section of a circular disk at normal incidence is four times as large for electromagnetic scattering as for sound scattering in the Rayleigh region. For back-scattering from a sphere the electromagnetic answer is nine times as large as the sound answer.

A case in which a correspondence between the electromagnetic problem and a scalar problem holds for all wavelengths is that of scattering from a cylinder. If the cylinder is perpendicular to the x-y plane and the incident radiation is polarized in the x-y plane, the electric field can be expressed as the curl of a vector which has only a z component. This component satisfies the scalar

<sup>1</sup> $\rho$  denotes the characteristic dimension of the body.

Helmholtz equation with a scalar Neumann boundary condition. Thus, this component corresponds to the velocity potential in sound scattering from a rigid body. If the incident radiation is polarized parallel to the z axis, the electric vector has only a z component. This component satisfies the scalar Helmholtz equation with a scalar Dirichlet boundary condition. Thus, for the type of body we are now discussing, due to the linearity of the equations, the field for the electromagnetic problem for arbitrary incident polarization can be obtained from the solutions of two independent scalar problems. These statements are in agreement with Reference 8 (an article on ripple tanks). It is stated therein, that an analogy between ripples and both acoustic and electromagnetic waves may be made when the electromagnetic problems can be stated in terms of scalar functions satisfying the scalar Helmholtz equation.

Another illustration of the correspondence between scalar and electromagnetic theory is presented in Section V of this paper for the case of back-scattering from a cone. The electromagnetic cross-section is shown to be greater than the sound cross-section by a factor which is independent of wavelength. The factor varies from four for a half-cone angle of  $0^\circ$  to one for a half-cone angle of  $90^\circ$ .

## III

SPECIAL SUMMATION TECHNIQUES

Before turning to the actual problem of determining the scattering cross-section for a cone, a few general comments on the nature of the analytic solution and the method by which this solution is made to yield numerical results are in order.

The original equation of the motion is hyperbolic. (The scalar scattering problem will be discussed to simplify the presentation.) This equation requires Cauchy conditions (two conditions at the boundary either in space or in time). However, since almost all the time dependences can be obtained from a linear combination of expressions of the form  $e^{-j\omega t}$  and since this type of time dependence can be used successfully to separate time out of the equation, the solution of the equation of the motion may be assumed without loss of generality to be the product of a function of space and  $e^{-j\omega t}$ .<sup>1</sup> This procedure allows one to obtain an elliptic differential equation in the space variables. One then applies a Neumann condition at the body and the Sommerfield radiation condition as the distance from the scatterer becomes "large".

This latter condition causes extreme difficulty. This difficulty is not in the nature of the physics of the scattering problem but in the nature of the mathematical description of the physics.<sup>2</sup> The physical problem under discussion has a finite source a large distance away which, when no scatterer is present, appears to the observer to produce plane waves. One then introduces a scatterer

---

<sup>1</sup>Throughout this paper  $j$  is used to denote  $\sqrt{-1}$ .

<sup>2</sup>The authors wish to thank Professor R. C. Bartels of the University of Michigan and Dr. C. L. Dolph of the Willow Run Research Center for their presentation of this viewpoint.



into the field. The observer now measures the total field. This total field consists of an incident plane wave and a scattered wave. Unfortunately, although making complete sense physically, the radiation condition applies only to the scattered field. Thus, it is the nature of the mathematical description of the radiation condition which forces the separation of the incident field from the scattered field. Such a separation is impossible physically because one cannot measure the scattered and incident waves individually. This separation causes (or forces) the functions of the distance variables to be broken up, when the distance becomes large, into forms that can be recognized as incoming and outgoing waves. This leads (or forces) the investigator to use asymptotic expressions which are applicable only when the distance variable represents a "large" distance from the scatterer. For an infinite cone it appears as though an essential ambiguity has been introduced into the problem because there is no characteristic dimension of an infinite cone compared with which the distance variable can be considered large. In this respect the cone problem is different from the previously solved three-dimensional problems.

In scattering problems special summation techniques may be applied to improve the rapidity of the convergence of the series solutions. When the characteristic dimension of a body is very large with respect to the wavelength,  $\lambda$ , one would expect that special summation techniques would facilitate the numerical evaluation of a solution, since the number of terms to be summed is greater than or equal to the ratio of the characteristic dimension to the wavelength. The latter fact may be illustrated by some simple examples. If  $\underline{m}$  represents the order of the highest order term required in the general summation, we have for sound scattering from a cylinder of radius  $\underline{a}$ , that

$$m \gg \frac{2\pi a}{\lambda}$$

and 
$$\left[ \frac{(m!)^2}{\pi m} \right]^{1/2m} \gg \frac{\pi a}{\lambda} .$$

Similarly, for sound scattering from a sphere of radius  $\underline{a}$ ,  $m \gg \frac{2\pi a}{\lambda}$

and

$$\left[ \frac{(2m+1)!}{2^m m!} \right]^{\frac{1}{m+1}} \gg \frac{2\pi a}{\lambda} .$$

This latter inequality is exactly the same as that obtained in collision theory in Quantum Mechanics (Ref. 10). For electromagnetic scattering from a perfectly conducting sphere of radius a we have (Ref. 11 and 12)<sup>1</sup>

$$m \geq \frac{2\pi a}{\lambda} .$$

In any case straight summation could be employed to obtain cross-sections as long as the ratio of characteristic dimension to wavelength is finite. However, as the characteristic dimension increases without limit (in the direction of propagation), the number of terms required for a meaningful solution increases without limit. This increase in the number of terms to be summed indicates that a special summation technique should be used if the ratio of characteristic dimension to wavelength is large. If the ratio of characteristic dimension to wavelength is without bound, a special summation technique must be used.

In any particular problem the choice of the type of summation technique to be employed must be governed by the nature of the mathematical expression of the problem and by the investigator's experience. The Euler method of summation (Ref. 13, p. 62) has been selected for use in the cone problem.

<sup>1</sup>The equals sign appears in Reference 11; however, the authors believe that it should be ≥.

## IV

THE WEDGE

The role of summation methods in obtaining the field scattered from the cone can be clarified by comparing the cone and the wedge solutions. For simplicity we will deal with scalar scattering and consider only the field along the axis of symmetry. For the cone the field is given by (see UMM-87)

$$u_c = \sqrt{\frac{2}{kr}} \sum_{i=0}^{\infty} \left(n_i + \frac{1}{2}\right) \frac{\sin\left(\frac{n_i \pi}{2}\right) e^{jn_i \pi/2} \Gamma\left(\frac{n_i + 1}{2}\right) J_{n_i + \frac{1}{2}}(kr)}{\sin\left(\frac{n_i \pi}{2}\right) \Gamma\left(\frac{n_i + 2}{2}\right) (1 - \mu_o^2) P_{n_i}(\mu_o) \frac{\partial^2 P_{n_i}(\mu_o)}{\partial n_i \partial \mu}} \quad (\text{IV-1})$$

where  $n_i$  is the  $(i + 1)$ th zero of  $P_{n_i}^1(\mu_o)$ ,  $\theta_1 = \pi - \theta_o$  is  $1/2$  the cone angle, and  $\mu_o = \cos \theta_o$ . The corresponding expression for the wedge (Ref. 3) is

$$u_w = 2 \frac{\pi}{\pi - \theta_2} \sum_{i=0}^{\infty} e^{-j \frac{\pi^2 i}{\pi - \theta_2}} J_{\frac{i\pi}{\pi - \theta_2}}(kr) \left[1 - \frac{1}{2} \delta_{i0}\right] \quad (\text{IV-2})$$

where  $\delta_{i0}$  is the Kronecker delta and  $\theta_2 = \frac{1}{2}$  the wedge angle.

Both of these series converge because of the rapidity with which  $J_\eta(kr)$  goes to zero as  $\eta$  goes to infinity when  $\eta \gg kr$ . To determine the behavior of the series for  $i \ll kr$ , it is convenient to use the appropriate asymptotic expression for the Bessel function. Using this asymptotic expression we find that the wedge series becomes

$$\begin{aligned}
 u_w = & 2 \frac{\pi}{\pi - \theta_2} \sqrt{\frac{2}{\pi k r}} \sum_{i=0}^{\ell \ll k r} e^{-j \frac{\pi^2 i}{\pi - \theta_2}} \\
 & \times \frac{\exp \left[ j \left( k r - \frac{\pi}{4} - \frac{i \pi^2}{2(\pi - \theta_2)} \right) \right] + \exp \left[ -j \left( k r - \frac{\pi}{4} - \frac{i \pi^2}{2(\pi - \theta_2)} \right) \right]}{2} \\
 & + 2 \frac{\pi}{\pi - \theta_2} \sum_{i=\ell+1}^{\infty} e^{-j \frac{\pi^2 i}{\pi - \theta_2}} J_{\frac{i \pi}{\pi - \theta_2}}(k r) - \frac{\pi}{\pi - \theta_2} \sqrt{\frac{2}{\pi k r}} \cos \left[ k r - \frac{\pi}{4} \right] + o\left(\frac{1}{k r}\right).
 \end{aligned}
 \tag{IV-3}$$

Thus, the initial terms of the series (IV-3) oscillate in magnitude with a constant maximum magnitude. The series, therefore, does not show signs of convergence when  $i \ll k r$ . For large  $k r$  the series may converge very slowly indeed. The situation is more complex for the case of the cone, but it is found that for  $i \ll k r$  the magnitude of each term of the series increases roughly linearly with  $i$ . Thus, the cone series also converges very slowly for large  $k r$ . These two series (the one for the cone and the one for the wedge) can be made more rapidly convergent by means of the following transformation (which is certainly legitimate since the two series are absolutely convergent):

$$\sum_{i=0}^{\infty} e^{a i j} V_i = \frac{1}{1 - e^{a j}} \left[ V_0 + \sum_{i=0}^{\infty} e^{a(i+1)j} \{V_{i+1} - V_i\} \right] \tag{IV-4}$$

Applying this transformation to the first sum appearing in (IV-3) and taking  $a = \frac{-3 \pi^2}{2(\pi - \theta_2)}$  and  $\frac{-\pi^2}{2(\pi - \theta_2)}$  respectively for the

two parts of that sum, one obtains:<sup>1</sup>

$$\begin{aligned}
 u_w = & \frac{\pi}{\pi - \theta_2} \sqrt{\frac{2}{\pi kr}} \left\{ \frac{\exp \left[ j \left( kr - \frac{\pi}{4} \right) \right]}{1 - \exp \left[ \frac{-3\pi^2 j}{2(\pi - \theta_2)} \right]} \right. \\
 & \times \left[ 1 + \sum_{i=0}^{\ell \ll kr} \left\{ \exp \left[ \frac{-3\pi^2 j (i+1)}{2(\pi - \theta_2)} \right] (1-1) \right\} \right] \\
 & + \exp \left[ -j \left( kr - \frac{\pi}{4} \right) \right] \left[ 1 + \sum_{i=0}^{\ell \ll kr} \left\{ \exp \left[ \frac{-\pi^2 j (i+1)}{2(\pi - \theta_2)} \right] (1-1) \right\} \right] \left. \right\} \\
 & - \frac{\pi}{\pi - \theta_2} \sqrt{\frac{2}{\pi kr}} \cos \left[ kr - \frac{\pi}{4} \right] + O \left( \frac{1}{kr} \right). \quad (IV-5)
 \end{aligned}$$

Thus the  $u_w$  series has been evaluated to within  $O(1/kr)$ .

The method of evaluating  $u_c$  is the same except that the transformation must be applied to the series twice.

<sup>1</sup>Although the portion of the  $u_w$  series from  $\ell$  to  $\infty$  is not indicated in (IV-5), it can be shown that (IV-4) transforms this portion of (IV-3) into a negligible quantity.

## V

THE CONE

In what follows the radar cross-section of a cone is discussed and the results obtained are compared with experiment. In Part A the analytic expressions for  $\sigma$  obtained from physical optics, scalar theory, and electromagnetic theory are considered. The physical optics form,  $\sigma_{p.o.}(0)$ , is merely stated, but the latter two are discussed in some detail. For the scalar case the discussion consists of two parts, the proof of the convergence of the series solution and the break up of the solution into an "incoming" and an "outgoing" part. The "outgoing" part yields the scalar cross-section  $\sigma(0)$ . The discussion of the electromagnetic theory result consists primarily of the methods used in expressing the result as a sum of an incoming plane wave and an outgoing wave which at large distances from the scattering body appears to be a spherical wave. Again this break up of the solution leads directly to the electromagnetic cross-section, which is denoted by  $\sigma'(0)$ .

Part B of this section contains the analysis involved in applying the special summation methods to the problem of finding  $\sigma(0)$  and  $\sigma'(0)$  for small cone angles. Part C contains a similar analysis for the large cone angles, and also an approach that might be used for any cone angle.

A THE ANALYTIC EXPRESSIONS FOR  $\sigma$ 

One of the aims of this paper is to compare the results obtained by the methods of physical optics with those obtained by electromagnetic theory. Thus, a few comments on the physical optics expression for  $\sigma$  are in order prior to discussing the exact methods. These comments need not be lengthy; in fact, it will suffice to quote the physical optics results obtained in Section II-A of UMM-87. Therein the well known "scattering from the tip" answer is derived and expressed as

$$\sigma_{\text{p.o.}}(0) = \frac{\lambda^2}{16\pi} \tan^4 \theta_1 \quad (\text{V-1})$$

with  $\theta_1$  equal to 1/2 the cone angle.

It was pointed out in the introduction that interest in the infinite cone is partially tied up with its connection with the finite ogive. If one applies the method of physical optics outlined in UMM-87, he finds that the back-scattering cross-section of an ogive of length  $\ell$  ( $d/\lambda \gg 1$ ) and 1/2 ogive-nose angle  $\theta_1$  ( $\theta_1 < \pi/2$ ) is given by<sup>1</sup>

$$\sigma \approx \frac{\lambda^2}{16\pi} \tan^4 \theta_1 \left\{ 1 + \frac{\cos^4 \theta_1}{(1 + \cos \theta_1)^2} + \frac{2 \cos^2 \theta_1 \cos\left(\frac{2\pi\ell}{\lambda}\right)}{1 + \cos \theta_1} \right\}. \quad (\text{V-2})$$

One can readily see that the two results, (V-1) and (V-2), are approximately equal.

In this discussion of the analytic expressions for  $\sigma$ , the scalar case will be considered next. As was pointed out in UMM-87, the solution,  $u$ , to the wave equation,  $\nabla^2 u + k^2 u = 0$ , consists of a finite number of terms; i.e., the series solution is convergent and thus can be approximated by a sum of a finite number of terms. The convergence is established as follows:

The solution of the wave equation for the scattering of sound waves from a cone is

$$u = 2 \sqrt{\frac{\pi}{2kr}} \sum_{i=0}^{\infty} \frac{e^{jn_i \pi/2} J_{n_i + \frac{1}{2}}(kr) P_{n_i}(\mu)}{\int_{\mu_0}^1 [P_{n_i}(\mu)]^2 d\mu}. \quad (\text{V-3})$$

(See UMM-87, p. 15).

<sup>1</sup>The derivation of this result will be included in a future report under the title "Theoretical Scattering Cross-Section as a Function of Angle at Small Wavelengths". This report will be published under another contract. The  $d$ , maximum diameter of the ogive, and  $\ell$  are related by the equation  $d = \ell \tan(\theta_1/2)$ .

Let  $kr$  be large but finite. To show that the above series is convergent it suffices to demonstrate the convergence of

$$\sum_{i=\ell[kr]+1}^{\infty} \frac{e^{jn_i\pi/2} J_{n_i+1/2}(kr) P_{n_i}(\mu)}{\int_{\mu_0}^1 [P_{n_i}(\mu)]^2 d\mu}, \quad 1$$

with  $\ell$  such that  $n_{\ell[kr]+1} \gg kr$  and  $\ell \gg 1$ .

We first note that

$$P_{n_i}(\cos \theta) \approx \sqrt{\frac{2}{\pi n_i \sin \theta}} \cdot \cos \left\{ \left( n_i + \frac{1}{2} \right) \theta - \frac{\pi}{4} \right\}$$

for large values of  $n_i$  and  $\epsilon \leq \theta \leq \pi - \epsilon$ ,  $\epsilon > 0$ ,  $n_i \gg \frac{1}{\epsilon}$  (Ref. 14, p. 71). Thus we obtain the inequality,

$$\begin{aligned} \int_{\mu_0}^1 [P_{n_i}(\mu)]^2 d\mu &> \int_{\pi-\theta_0}^{\theta_0} [P_{n_i}(\cos \theta)]^2 \sin \theta d\theta \\ &> \frac{2}{\pi n_i} \int_{\pi-\theta_0}^{\theta_0} \cos^2 \left[ \left( n_i + \frac{1}{2} \right) \theta - \frac{\pi}{4} \right] d\theta \\ &> \frac{2\theta_0 - \pi}{\pi n_i} + O\left(\frac{1}{n_i^2}\right). \end{aligned} \quad (V-4)$$

From page 498 of Reference 15 (also Ref. 14. p. 25)

$$J_{n_i+1/2}(kr) \approx \frac{\left(\frac{kr}{2}\right)^{n_i+1/2}}{\Gamma\left(n_i+\frac{3}{2}\right)}, \quad n_i \gg kr$$

<sup>1</sup>[ $kr$ ] denotes the largest integer in  $kr$ .



which can be expressed in the form

$$J_{n_i + \frac{1}{2}}(kr) \approx \frac{\left(\frac{kre}{2n_i + 1}\right)^{n_i} \left(\frac{kre}{2}\right)^{1/2}}{\sqrt{2\pi} (n_i + 1/2)} \quad (V-5)$$

when the asymptotic form of  $\Gamma(z)$  (Ref. 14, p. 4) is employed. Using (V-4) and (V-5) and the fact that  $|P_{n_i}(\mu)| \leq 1$  for the values of  $\mu$  of interest, one obtains the inequality

$$\sum_{i=\ell[kr]+1}^{\infty} \left| \frac{e^{n_i \pi j / 2} J_{n_i + \frac{1}{2}}(kr) P_{n_i}(\mu)}{\int_{\mu_0}^1 [P_{n_i}(\mu)]^2 d\mu} \right| < \sum_{i=\ell[kr]+1}^{\infty} \frac{(kre\pi)^{1/2}}{2(2\theta_0 - \pi)} \left(\frac{kre}{2n_i + 1}\right)^{n_i} \quad (V-6)$$

Since  $i < (n_i + 1/2)$  in this region

$$\begin{aligned} \sum_{i=\ell[kr]+1}^{\infty} \left(\frac{kre}{2n_i + 1}\right)^{n_i} &< \sum_{i=\ell[kr]+1}^{\infty} \left(\frac{kre}{2i}\right)^{n_i} \\ &< \sum_{i=\ell[kr]+1}^{\infty} \left(\frac{e}{2\ell}\right)^{n_i} \end{aligned} \quad (V-7)$$

$$\text{But } \sum_{i=\ell[kr]+1}^{\infty} (e/2\ell)^{n_i} < \int_{\ell[kr]}^{\infty} (e/2\ell)^x dx = -\frac{(e/2\ell)^{\ell[kr]}}{\ln(e/2\ell)} \quad (V-8)$$

Thus, if we use (V-6), (V-7), and (V-8), we find that

$$\sum_{i=\ell[kr]+1}^{\infty} \left| \frac{e^{n_i \pi j / 2} J_{n_i + \frac{1}{2}}(kr) P_{n_i}(\mu)}{\int_{\mu_0}^1 [P_{n_i}(\mu)]^2 d\mu} \right|$$

$$< \frac{(kre\pi)^{1/2}}{2(2\theta_0 - \pi)} \left( \frac{-(e/2\ell)^{\ell[kr]}}{\log_e (e/2\ell)} \right). \quad (V-9)$$

The convergence of the integral in (V-8) implies the absolute convergence of the original series. Since we wish to conclude that the series can be given by a sum of a finite number of terms, it is informative to get an idea of the magnitude of the upper bound indicated in (V-9). If  $\ell = 100$  and  $kr = 10^6$  (which are reasonable values) this upper bound has the value

$$\frac{(e\pi)^{1/2} \times 10^3}{2(2\theta_0 - \pi)} \times \frac{(e/200)^{10^8}}{\log_e (200/e)}$$

which is much less than  $1/(\theta_0 - \pi/2) 10^{10^7}$ . Therefore, it is obvious that the sum from 100 [kr] to  $\infty$  is much less than 1 if

$(\theta_0 - \frac{\pi}{2}) > 10^{-(10^7-2)}$ . Thus, we can conclude that with  $\ell = 100$  the sum in (V-3) is approximately given by

$$2\sqrt{\frac{\pi}{2kr}} \sum_{i=0}^{100[kr]} \frac{e^{n_i \pi j / 2} J_{n_i + \frac{1}{2}}(kr) P_{n_i}(\mu)}{\int_{\mu_0}^1 [P_{n_i}(\mu)]^2 d\mu} \quad (V-10)$$

under the assumption that (V-10) is large in comparison to the upper bound computed above. One cannot at this point rule out the possibility that the sum in (V-10) is of the same order of magnitude or less than the upper bound as defined in (V-9). However,

the computations which follow in Parts B and C of this section show that the assumption that (V-3) and (V-10) are approximately equal is in fact a valid one. Thus, not only can we conclude that the series in (V-3) converges but also that it can be considered to be given by a sum of only a finite number of terms.

The next step is to obtain explicitly the differential scattering coefficient for the cone. In order to do this, the solution must be broken up at large  $kr$  into an incoming and an outgoing part, i.e., in the limit as  $kr \rightarrow \infty$ .

$$u \approx e^{jkr \cos \theta} + \frac{f(\theta)}{r} e^{-jkr}$$

It is the coefficient,  $f(\theta)$ , of the outgoing part of the solution that is the differential scattering coefficient, and we may write in the limit as  $kr \rightarrow \infty$ ,

$$f(\theta) = \frac{r}{e^{-jkr}} \left\{ u(r, \theta) - e^{jkr \cos \theta} \right\}$$

$$= \frac{r}{e^{-jkr}} \left\{ 4 \sqrt{\frac{\pi}{2kr}} \sum_{i=0}^{\infty} \frac{(n_i + 1/2) e^{jn_i \pi/2} J_{n_i + \frac{1}{2}}(kr) P_{n_i}(\mu)}{(1 - \mu_o^2) P_{n_i}(\mu) \frac{\partial^2 P_{n_i}(\mu_o)}{\partial n_i \partial \mu}} - \sum_{i=0}^{\infty} a_i(kr) P_{n_i}(\mu) \right\} \quad (V-11)$$

The plane wave  $e^{jkr \cos \theta}$  has been written symbolically as an expansion in the  $P_{n_i}$ 's with coefficient  $a_i(kr)$ . The summation method will be applied to the first few terms of the above expression. The justification for doing this lies in the fact that the numerical values

---

<sup>1</sup>In the discussion of the scalar case the time dependence defined by  $e^{j\omega t}$  is used.

obtained after applying the summation method decrease very rapidly after the first few terms. Since (V-11) is convergent, the result obtained by using only the first few terms represents the entire series. In UMM-87 the asymptotic form of (V-11) is given as

$$f(\theta) = \frac{j}{k} \sum_{i=0}^{\infty} \frac{e^{jn_i\pi} P_{n_i}(\mu)}{\int_{\mu_0}^1 [P_{n_i}(\mu)]^2 d\mu},$$

where no upper limit is given on the summation since approximately  $\sqrt{kr}/100$  terms of the series will have the form shown above and the remaining terms do not contribute to the value of  $f(\theta)$  when the summation method is employed.

For back-scattering one may write the differential scattering cross-section as

$$\sigma_D(0) = |f(\theta)|^2 = \frac{1}{k^2} \left| \sum_{i=0}^{\infty} \frac{e^{jn_i\pi}}{\int_{\mu_0}^1 [P_{n_i}(\mu)]^2 d\mu} \right|^2. \quad (V-12)$$

For the vector case (Ref. 5)<sup>1</sup> the situation is analogous to the scalar case. In this case, there are two sums throughout since the vector potential  $\vec{A}(\vec{r})$ , which must be constructed from the two linearly independent vector solutions  $\vec{m}$  and  $\vec{n}$ , is used (Ref. 11, p. 414). If the situation is as depicted in Figure V-1, and with the incident plane wave polarized in the x-direction, then

<sup>1</sup>The notation of Hansen and Schiff is employed throughout this discussion of the vector case. It should be noted that spherical coordinates are used and  $z_x(kr)$  denotes the spherical Bessel function.

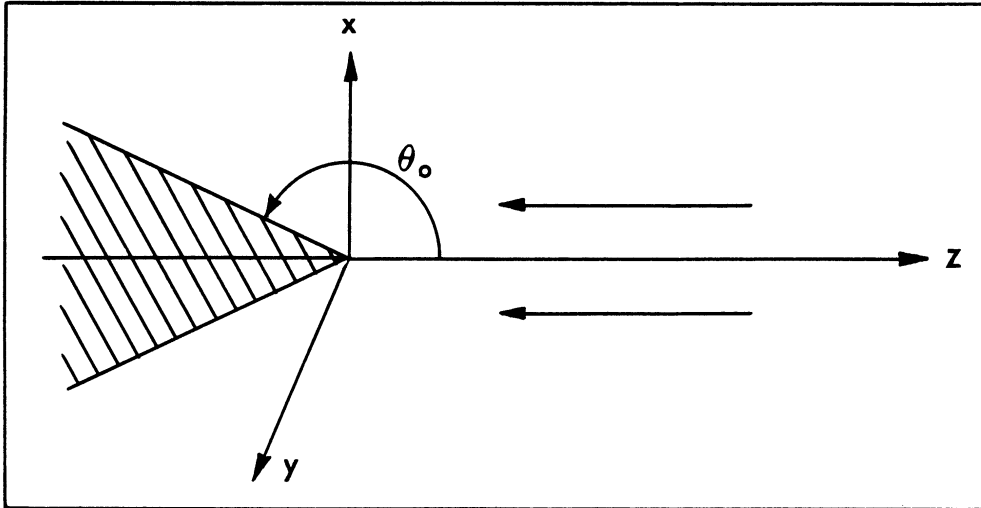


FIG. V-1 GEOMETRY OF SCATTERING FROM AN INFINITE CONE

$$\begin{aligned}
 \vec{A}(\vec{r}) &= \sum_{i=0}^{\infty} a_{n_i} \vec{m}_{0,1,n_i} + \sum_{i=0}^{\infty} \beta_{m_i} \vec{n}_{e,1,m_i} \\
 &= \hat{i}_\theta \left\{ \sum_{i=0}^{\infty} a_{n_i} \frac{P_{n_i}^1(\mu)}{\sin \theta} z_{n_i}(kr) \cos \phi \right. \\
 &\quad \left. - \sum_{i=0}^{\infty} \beta_{m_i} \frac{dP_{m_i}^1(\mu)}{d\theta} \left[ \frac{1}{kr} \frac{\partial}{\partial r} [rz_{m_i}(kr)] \right] \cos \phi \right\} \\
 &+ \hat{i}_\phi \left\{ - \sum_{i=0}^{\infty} a_{n_i} \frac{dP_{n_i}^1(\mu)}{d\theta} z_{n_i}(kr) \sin \phi \right. \\
 &\quad \left. + \sum_{i=0}^{\infty} \beta_{m_i} \frac{P_{m_i}^1(\mu)}{\sin \theta} \left[ \frac{1}{kr} \frac{\partial}{\partial r} [rz_{m_i}(kr)] \right] \sin \phi \right\} \\
 &+ \hat{i}_r \left\{ \sum_{i=0}^{\infty} \frac{m_i(m_i+1)}{kr} z_{m_i}(kr) P_{m_i}^1(\mu) \cos \phi \right\} \quad (V-13)
 \end{aligned}$$

where the boundary condition (tangential component of the vector potential is zero on the surface of the cone) determines the  $n_i$ 's and  $m_i$ 's according to the relations

$$P_{n_i}^1(\cos \theta_0) = 0 \quad \text{and} \quad \left. \frac{dP_{m_i}^1(\mu)}{d\mu} \right|_{\mu=\cos \theta_0} = 0.$$

Since  $\alpha_{n_i}$  and  $\beta_{m_i}$  are independent of  $\theta$ ,  $\phi$ , and  $r$ , let us consider the special case  $\theta = 0$  since we are interested only in back-scattering. Using the relations

$$\left. \frac{dP_{n_i}^1(\mu)}{d\theta} \right|_{\theta=0} = \frac{1}{2} n_i(n_i + 1) \quad \text{and} \quad \left. \frac{P_{n_i}^1(\mu)}{\sin \theta} \right|_{\theta=0} = \frac{1}{2} n_i(n_i + 1)$$

we find that

$$\begin{aligned} \vec{A}(r, 0) = \hat{i}_x \left\{ \sum_{i=0}^{\infty} \alpha_{n_i} z_{n_i}(kr) \frac{n_i(n_i + 1)}{2} \right. \\ \left. - \sum_{i=0}^{\infty} \beta_{m_i} \frac{1}{kr} \left[ \frac{\partial}{\partial r} (r z_{m_i}(kr)) \right] \frac{m_i(m_i + 1)}{2} \right\}. \end{aligned} \tag{V-14}$$

For  $\theta = 0$  the plane wave polarized in the x-direction is  $\hat{i} e^{-jkz}$ . At large  $kr$  we require that the total wave minus the plane wave (which is shown in Ref. 5 to be only incoming) have the form of an outgoing wave. The plane wave has the form

$$\sum_i \alpha_{n_i}(kr) \frac{n_i(n_i + 1)}{2} + \sum_i g_{m_i}(kr) \frac{m_i(m_i + 1)}{2}$$

where in the limit as  $kr \rightarrow \infty$

$$a_{n_i}(kr) \longrightarrow \frac{je^{-jkr}}{B_{n_i}(kr)} \quad \text{and} \quad g_{m_i}(kr) \longrightarrow \frac{je^{-jkr}}{B_{m_i}(kr)}$$

and

$$B_{n_i} = \int_{\mu_0}^1 [P_{n_i}^1(\mu)]^2 d\mu \quad \text{and} \quad B_{m_i} = \int_{\mu_0}^1 [P_{m_i}^1(\mu)]^2 d\mu.$$

Thus, we require

$$\begin{aligned} & \sum_{i=0}^{\infty} a_{n_i} z_{n_i}(kr) \frac{n_i(n_i + 1)}{2} - \sum_{i=0}^{\infty} a_{n_i}(kr) \frac{n_i(n_i + 1)}{2} \\ & + \sum_{i=0}^{\infty} \beta_{m_i} \frac{1}{kr} \frac{\partial}{\partial r} \left( r z_{m_i}(kr) \right) \frac{m_i(m_i + 1)}{2} \\ & - \sum_{i=0}^{\infty} g_{m_i}(kr) \frac{m_i(m_i + 1)}{2} = \text{outgoing wave.} \end{aligned}$$

We only know how to break up the spherical Bessel functions explicitly into outgoing and incoming parts when we can replace them by their asymptotic forms valid for  $\sqrt{kr} \gg n_i$  or  $m_i$ . Thus, we break up the sums into two parts, from  $i = 0$  to  $[\sqrt{kr}/100]$  and from  $[\sqrt{kr}/100] + 1$  to  $\infty$ .

Thus

$$\begin{aligned} & \sum_0^{[\sqrt{kr}/100]} (a_{n_i})_1 z_{n_i}(kr) \underline{\underline{\text{in}}} \frac{n_i(n_i+1)}{2} - \sum_0^{[\sqrt{kr}/100]} a_{n_i}(kr) \frac{n_i(n_i+1)}{2} \\ & + \sum_0^{[\sqrt{kr}/100]} (a_{n_i})_1 z_{n_i}(kr) \underline{\underline{\text{out}}} \frac{n_i(n_i+1)}{2} + \sum_{[\sqrt{kr}/100+1]}^{\infty} (a_{n_i})_2 z_{n_i}(kr) \underline{\underline{\text{in}}} \frac{n_i(n_i+1)}{2} \\ & - \sum_{[\sqrt{kr}/100+1]}^{\infty} a_{n_i}(kr) \frac{n_i(n_i+1)}{2} + \sum_{[\sqrt{kr}/100+1]}^{\infty} (a_{n_i})_2 z_{n_i}(kr) \underline{\underline{\text{out}}} \frac{n_i(n_i+1)}{2} \end{aligned}$$

+ similar terms in  $\beta_{m_i}$  and  $g_{m_i}(kr)$  = purely outgoing wave.

(V-15)

Since neither  $a_{n_i}(kr)$  nor  $g_{m_i}(kr)$  change in form over the entire range  $i = 0$  to  $i = \infty$ , then we have

$$\begin{aligned} & \sum_0^{[\sqrt{kr}/100]} (a_{n_i})_1 z_{n_i}(kr) \underline{\underline{\text{in}}} \frac{n_i(n_i+1)}{2} = \sum_0^{[\sqrt{kr}/100]} a_{n_i}(kr) \frac{n_i(n_i+1)}{2} \\ & \sum_{[\sqrt{kr}/100+1]}^{\infty} (a_{n_i})_2 z_{n_i}(kr) \underline{\underline{\text{in}}} \frac{n_i(n_i+1)}{2} = \sum_{[\sqrt{kr}/100+1]}^{\infty} a_{n_i}(kr) \frac{n_i(n_i+1)}{2} \end{aligned}$$

and two similar equations in  $\beta_{m_i}$  and  $g_{m_i}(kr)$ .



The first two equations imply that  $(\alpha_{n_i})_1 = (\alpha_{n_i})_2 = \alpha_{n_i}$ . Substituting the asymptotic forms for  $a_{n_i}(kr)$  and for the Bessel functions (in the limit as  $kr \rightarrow \infty$ ):

$$z_{n_i}(kr) \approx \frac{1}{kr} \cos\left(kr - \frac{n_i + 1}{2} \pi\right)$$

$$\frac{1}{kr} \frac{\partial}{\partial r} [rz_{n_i}(kr)] \approx \frac{1}{kr} \sin\left(kr - \frac{n_i + 1}{2} \pi\right).$$

We obtain  $\alpha_{n_i} = \frac{2}{B_{n_i}} e^{-jn_i\pi/2}$ . Similarly the two equations containing  $\beta_{m_i}$  and  $g_{m_i}(kr)$  give  $\beta_{m_i} = \frac{2j}{B_{m_i}} e^{-jm_i\pi/2}$ .

Since  $\alpha_{n_i}$  and  $\beta_{m_i}$  are independent of  $kr$  they are correct for all  $kr$ , and (V-14) takes on the form

$$\vec{A}(r, 0) = \hat{i}_x \left\{ \sum_{i=0}^{\infty} \frac{1}{B_{n_i}} e^{-jn_i\pi/2} z_{n_i}(kr) n_i (n_i + 1) - \sum_{i=0}^{\infty} \frac{j}{B_{m_i}} e^{-jm_i\pi/2} \frac{1}{kr} \frac{\partial}{\partial r} [rz_{m_i}(kr)] m_i (m_i + 1) \right\} \quad (V-16)$$

By exactly the same procedure used in the scalar case, it can be seen that the two series are convergent. Just as in the scalar case the coefficient of the outgoing wave may be written (for the back-scattering case) as

UMM-92

$$\begin{aligned}
 f(0) \frac{e^{jkr}}{r} &\approx \left\{ \left| \vec{A}(r, 0) \right| - e^{-jkz} \right\} \approx \sum_{i=0}^{\infty} \frac{e^{-jn_i\pi/2}}{B_{n_i}} z_{n_i}(kr) n_i (n_i + 1) \\
 &- \sum_{i=0}^{\infty} \frac{je^{-jm_i\pi/2}}{B_{m_i}} \frac{1}{kr} \frac{\partial}{\partial r} \left\{ rz_{m_i} \right\} m_i (m_i + 1) \\
 &- \sum_{i=0}^{\infty} a_{n_i}(kr) \frac{n_i(n_i+1)}{2} - \sum_{i=0}^{\infty} g_{m_i}(kr) \frac{m_i(m_i+1)}{2}
 \end{aligned} \tag{V-17}$$

Again, the summation method will be applied only to the first few terms of  $f(0)$ . Using the appropriate asymptotic forms we get

$$\begin{aligned}
 \sigma'_D(0) &= \left| f(0) \right|^2 = \\
 &\frac{1}{k^2} \left| \sum_i \frac{n_i(n_i+1)}{2B_{n_i}} e^{-jn_i\pi} - \sum_i \frac{m_i(m_i+1)}{2B_{m_i}} e^{-jm_i\pi} \right|^2
 \end{aligned} \tag{V-18}$$

where no upper limit is given on the sums to indicate that approximately  $\sqrt{kr}/100$  terms of the series will have the form shown and the remaining terms do not contribute to the sum when the summation method is employed.

## B $\sigma$ FOR SMALL CONE ANGLES

It has been shown on the preceding pages that the nose-on radar cross-sections of a semi-infinite cone for the cases of vector and scalar scattering are given by<sup>1</sup>

<sup>1</sup>Note that  $\sigma = 4\pi\sigma_D$ .

$$\sigma'(0) = \frac{\lambda^2}{4\pi} \left| \sum_{i=0} \frac{n_i(n_i+1) e^{j\pi n_i}}{B_{n_i}} - \frac{m_i(m_i+1) e^{j\pi m_i}}{B_{m_i}} \right|^2 \quad (\text{see footnote } ^1)$$

$$\sigma(0) = \frac{\lambda^2}{\pi} \left| \sum_{i=0} \frac{n_i(n_i+1) e^{j\pi n_i}}{B_{n_i}} \right|^2 \quad (\text{V-19})$$

The "i = 0 term" in  $\sigma'(0)$  series vanishes and the "i = 0 term" in the  $\sigma(0)$  series is equal to  $1/(1 + \cos \theta_1)$ . This term is used in the final evaluation of the scalar cross-section, but the discussion which follows relative to approximating the  $n_i$ 's and the  $m_i$ 's is restricted to  $i \geq 1$ .

Letting  $\theta_1$  denote 1/2 of the total cone angle we have  $\theta_1 = \pi - \theta_0$ . Then, by means of a formula given by Schelkunoff (Ref. 16, p. 54), it is possible to obtain expressions for the cross-section valid for small cone angles. The formula is

$$P_\eta [\cos (\pi - \theta_1)] = \frac{\sin \eta \pi}{\pi} \sum_{s=0}^{\infty} \frac{(-1)^s \Gamma (\eta + 1 + s)}{(s!)^2 \Gamma (\eta + 1 - s)} [\ln \delta + \psi (\eta + s)$$

$$+ \psi (\eta - s) - 2 \psi (s)] \delta^2 + \cos \eta \pi \sum_{s=0}^{\infty} \frac{(-1)^s \Gamma (\eta + 1 + s) \delta^s}{(s!)^2 \Gamma (\eta + 1 - s)}$$

(V-20)

where  $\delta = \frac{1 - \cos \theta_1}{2}$

<sup>1</sup>An independent method was used as a check on the summation method employed in this paper. In this independent approach the sum in  $\sigma'(0)$  is expressed as an integral and then it is seen that the sum itself is real. The details of this investigation appear in Appendix D.

and 
$$\psi(x) = \frac{d}{dx} \ln [\Gamma(x+1)].$$

Using this formula and the relation  $P_{\eta}^1(x) = -\sqrt{1-x^2} \frac{dP_{\eta}(x)}{dx}$  we find that

$$n_i = i \left[ 1 + (i+1)\delta + (i+1) \left\{ i(i+1) \left( \ln \delta + 2 \sum_{k=1}^i \frac{1}{k} \right) - \frac{1}{2} (i-1)(3i+2) \right\} \delta^2 + o(\delta^2) \right],$$

$$m_i = i \left[ 1 - (i+1)\delta + (i+1) \left\{ i(i+1) \left( \ln \delta + 2 \sum_{k=1}^i \frac{1}{k} \right) + \frac{1}{2} (i+2)(5i-1) \right\} \delta^2 + o(\delta^2) \right] \quad (V-21)$$

where  $i = 1, 2, 3$ , and  $o(\delta^2)$  is a function satisfying  $\lim_{\delta \rightarrow 0} \frac{o(\delta^2)}{\delta^2} = 0$ .

In addition

$$2 \frac{n_i(n_i+1)}{B_{n_i}} = (2i+1) + (6i^2 + 6i + 1)\delta + \left[ 2i(i+1)(5i^2 + 5i + 1) \left( \ln \delta + 2 \sum_{k=1}^i \frac{1}{k} \right) + i^2(i+1)^2(2i+1) \left( \frac{\pi^2}{3} - 2 \sum_{k=1}^i \frac{1}{k^2} \right) - (15i^4 + 10i^3 - 12i^2 - 9i - 1) \right] \delta^2 + o(\delta^2)$$

$$\begin{aligned}
 & 2 \frac{m_i (m_i + 1)}{B_{m_i}} = (2i + 1) - (6i^2 + 6i + 1) \delta \\
 & + \left[ 2i (i + 1) (5i^2 + 5i + 1) \left( \ln \delta + 2 \sum_{k=1}^i \frac{1}{k} \right) \right. \\
 & + i^2 (i + 1)^2 (2i + 1) \left( \frac{\pi^2}{3} - 2 \sum_{k=1}^i \frac{1}{k^2} \right) \\
 & \left. + (25i^4 + 70i^3 + 48i^2 + 5i - 1) \right] \delta^2 + o(\delta^2). \quad (V-22)
 \end{aligned}$$

If the above expressions are substituted into the cross-section formulas (V-19), expansions of the cross-sections are obtained which are valid for small angle cones. In order to obtain these expressions it is necessary to sum a number of series. The series

are of the form  $\sum_{n=1}^{\infty} (-1)^n n^m$ ,  $\sum_{n=1}^{\infty} \sum_{k=1}^n (-1)^n n^m \frac{1}{k}$ , and

$\sum_{n=1}^{\infty} \sum_{k=1}^n (-1)^n n^m \frac{1}{k^2}$  where  $m = 0, 1, 2, \dots$ . Using the formula

$$\sum_{n=1}^{\infty} (-1)^n V_n = -\frac{1}{2} \left[ V_1 + \sum_{n=1}^{\infty} (-1)^n (V_{n+1} - V_n) \right]$$

the following values of the necessary series are obtained:

$$\sum_{n=1}^{\infty} (-1)^n = -\frac{1}{2}$$

$$\sum_{n=1}^{\infty} (-1)^n n = -\frac{1}{2} \left[ 1 + \sum_{n=1}^{\infty} (-1)^n \right] = -\frac{1}{4}$$

$$\sum_{n=1}^{\infty} (-1)^n n^2 = -\frac{1}{2} \left[ 1 + \sum_{n=1}^{\infty} (-1)^n (2n+1) \right] = 0$$

$$\sum_{n=1}^{\infty} (-1)^n n^3 = \frac{1}{8}, \quad \sum_{n=1}^{\infty} (-1)^n n^4 = 0, \quad \sum_{n=1}^{\infty} (-1)^n n^5 = -\frac{1}{4}$$

$$\sum_{n=1}^{\infty} \sum_{k=1}^n (-1)^n \frac{1}{k} = \sum_{k=1}^{\infty} \sum_{n=k}^{\infty} (-1)^n \frac{1}{k} = -\frac{1}{2} \sum_{k=1}^{\infty} (-1)^{k-1} \frac{1}{k} = -\frac{1}{2} \ln 2$$

$$\sum_{n=1}^{\infty} \sum_{k=1}^n (-1)^n n \frac{1}{k} = -\frac{1}{2} \left[ 1 + \sum_{n=1}^{\infty} \sum_{k=1}^n (-1)^n \frac{1}{k} + \sum_{n=1}^{\infty} (-1)^n \right] = -\frac{1}{4} + \frac{1}{4} \ln 2$$

$$\sum_{n=1}^{\infty} \sum_{k=1}^n (-1)^n n^2 \frac{1}{k} = -\frac{1}{2} \left[ 1 + \sum_{n=1}^{\infty} \sum_{k=1}^n (-1)^n (2n+1) \frac{1}{k} + \sum_{n=1}^{\infty} (-1)^n (n+1) \right] = \frac{1}{8}$$

$$\sum_{n=1}^{\infty} \sum_{k=1}^n (-1)^n n^3 \frac{1}{k} = \frac{3}{16} - \frac{1}{8} \ln 2$$

$$\sum_{n=1}^{\infty} \sum_{k=1}^n (-1)^n n^4 \frac{1}{k} = -\frac{3}{16}$$

$$\sum_{n=1}^{\infty} \sum_{k=1}^n (-1)^n n^5 \frac{1}{k} = -\frac{15}{32} + \frac{1}{4} \ln 2$$

$$\sum_{n=1}^{\infty} \sum_{k=1}^n (-1)^n \frac{1}{k^2} = \sum_{k=1}^{\infty} \sum_{n=k}^{\infty} (-1)^n \frac{1}{k^2} = -\frac{1}{2} \sum_{k=1}^{\infty} (-1)^{k-1} \frac{1}{k^2} = -\frac{\pi^2}{24}$$

$$\sum_{n=1}^{\infty} \sum_{k=1}^n (-1)^n n \frac{1}{k^2} = -\frac{1}{2} \left[ 1 + \sum_{n=1}^{\infty} \sum_{k=1}^n (-1)^n \frac{1}{k^2} + \sum_{n=1}^{\infty} (-1)^n \frac{1}{n+1} \right]$$

$$= \frac{\pi^2}{48} - \frac{1}{2} \ln 2$$

$$\sum_{n=1}^{\infty} \sum_{k=1}^n (-1)^n n^2 \frac{1}{k^2} = -\frac{1}{2} \left[ 1 + \sum_{n=1}^{\infty} \sum_{k=1}^n (-1)^n (2n+1) \frac{1}{k^2} + \sum_{n=1}^{\infty} (-1)^n \right]$$

$$= -\frac{1}{4} + \frac{1}{2} \ln 2$$

$$\sum_{n=1}^{\infty} \sum_{k=1}^n (-1)^n n^3 \frac{1}{k^2} = \frac{1}{4} - \frac{\pi^2}{96}, \quad \sum_{n=1}^{\infty} \sum_{k=1}^n (-1)^n n^4 \frac{1}{k^2} = \frac{1}{4} - \frac{1}{2} \ln 2$$

$$\sum_{n=1}^{\infty} \sum_{k=1}^n (-1)^n n^5 \frac{1}{k^2} = -\frac{9}{16} + \frac{\pi^2}{48}.$$

Using these sums the final expressions for the cross-sections become

$$\sigma'(0) = \frac{\lambda^2 \delta^2}{\pi} \left[ 1 + 6\delta + \dots \right]$$

$$\sigma(0) = \frac{\lambda^2 \delta^2}{4\pi} \left[ 1 + \left( 4 \ln \frac{1}{\delta} - 2 \right) \delta + \dots \right]. \quad (\text{V-23})$$

It is interesting to compare these results with the physical optics expression for the cross-section,

$$\sigma_{\text{p.o.}}(0) = \frac{\lambda^2 \tan^4 \theta_1}{16\pi} = \frac{\lambda^2 \delta^2 (1 - \delta)^2}{\pi (1 - 2\delta)^4} = \frac{\lambda^2 \delta^2}{\pi} [1 + 6\delta + \dots]. \quad (\text{V-24})$$

$$\text{Clearly } 4 \lim_{\delta \rightarrow 0} \frac{\pi \sigma(0)}{\lambda^2 \delta^2} = \lim_{\delta \rightarrow 0} \frac{\pi \sigma'(0)}{\lambda^2 \delta^2} = \lim_{\delta \rightarrow 0} \frac{\pi \sigma_{\text{p.o.}}(0)}{\lambda^2 \delta^2}. \quad \text{The}$$

three expressions are compared in Figure V-2 for half cone angles from  $0^\circ$  to  $35^\circ$ .

C  $\sigma$  FOR OTHER CONE ANGLES

In using (V-19) to determine either  $\sigma'(0)$  or  $\sigma(0)$  it is necessary to find the values of the parameters  $n_i$ ,  $m_i$ ,  $B_{n_i}$ , and  $B_{m_i}$ . An approximation technique for the determination of these quantities was developed at the Willow Run Research Center and originally presented in References 17 and 18. A discussion of this technique and its application to the case  $\theta_0 = \pi - \theta_1 = 165^\circ$  appears in Appendix A.

The summation technique employed in finding  $\sigma$  is extremely sensitive to the first few values of these parameters. Hence, the errors resulting from this approximation method are greatly magnified by errors in the values of the four parameters. The Institute of Numerical Analysis (I.N.A.) of the University of California at Los Angeles has considered the problem of the determination of the parameters and has found these values to a greater degree of precision than can be obtained from the approximation techniques indicated in Appendix A.

If the parameters  $n_i$ ,  $m_i$ ,  $B_{n_i}$ , and  $B_{m_i}$  are given, the cross-section of a cone can be determined as follows:

The scalar and vector cross-sections are given by

$$\begin{aligned} \sigma(0) &= \frac{\lambda^2}{\pi} \left| \frac{1}{1 + \cos \theta_1} + \sum_{i=1} \frac{n_i(n_i + 1)}{B_{n_i}} e^{\pi n_i j} \right|^2 \\ \sigma'(0) &= \frac{\lambda^2}{4\pi} \left| \sum_i \left\{ \frac{n_i(n_i + 1) e^{\pi n_i j}}{B_{n_i}} - \frac{m_i(m_i + 1) e^{\pi m_i j}}{B_{m_i}} \right\} \right|^2. \quad \text{(V-19)} \end{aligned}$$



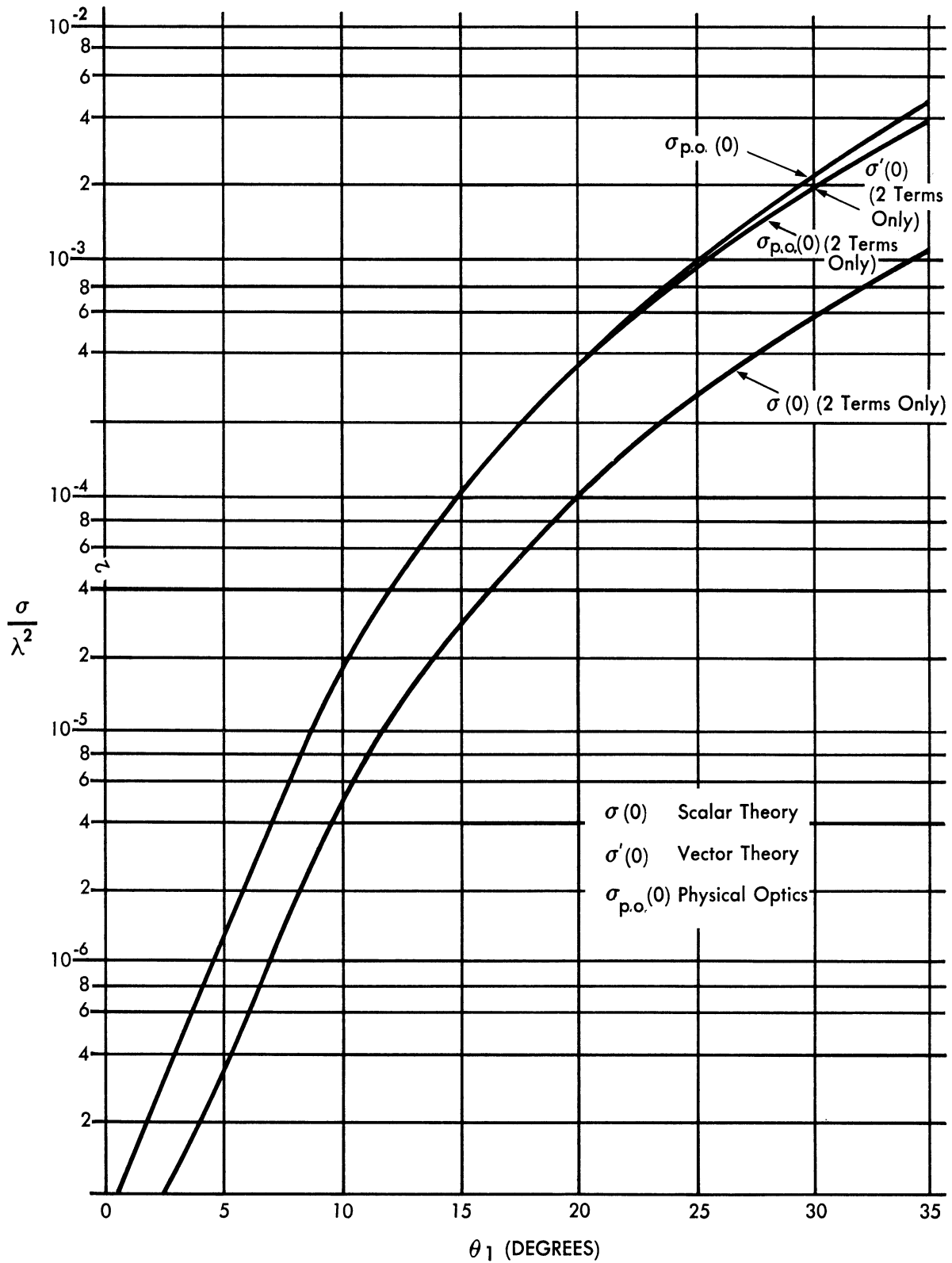


FIG. V - 2 COMPARISON BETWEEN  $\sigma'(0)$ ,  $\sigma(0)$ ,  $\sigma_{p.o.}(0)$  FOR THE "SMALL CONE ANGLE" APPROXIMATIONS

This method for summing these series will be illustrated only for the  $\sigma(0)$  series since the method is exactly the same for the  $\sigma'(0)$  series. The summation method is based on the Euler transformation

$$\sum_{i=1} e^{iaj} V_i = \sum_{n=0} \left( \frac{e^{ja}}{1 - e^{ja}} \right)^{n+1} \Delta^n V_1 \quad (V-25)$$

where

$$\Delta f_n = f_{n+1} - f_n$$

and

$$\Delta^m f_n = \Delta(\Delta^{m-1} f_n).$$

Since for large  $i$ ,  $n_{i+1} - n_i \approx m_{i+1} - m_i \approx \frac{\pi}{\pi - \theta_1}$ , it is most convenient to choose  $a = \frac{\pi^2}{\pi - \theta_1}$ . This choice ensures that  $\Delta^n V_1$  approaches zero rapidly as  $n$  increases and that the transformed series is rapidly convergent. The  $n_i$  series transforms as follows:

$$\begin{aligned} & \sum_{i=1} \frac{n_i(n_i + 1) \exp \left[ j\pi \left( n_i - \frac{\pi i}{\pi - \theta_1} \right) \right]}{B_{n_i}} e^{j \left( \frac{\pi^2 i}{\pi - \theta_1} \right)} \\ &= \sum_{k=0} \left\{ \frac{e^{j\pi^2/(\pi - \theta_1)}}{1 - e^{\pi^2 j/(\pi - \theta_1)}} \right\}^{k+1} \Delta^k \left\{ \frac{n_1(n_1 + 1) \exp \left[ \pi j \left( n_1 - \frac{\pi}{(\pi - \theta_1)} \right) \right]}{B_{n_1}} \right\} \end{aligned}$$

When the series has been evaluated, it is substituted into the cross-section expression.

If this method is applied using the values of the parameters computed by the technique of Appendix A, we find that for  $\theta_1 = 15^\circ$

$$\begin{aligned} \frac{\sigma'(0)}{\lambda^2} &= 2 \times 10^{-4} \\ \frac{\sigma(0)}{\lambda^2} &= 1.3 \times 10^{-4} \end{aligned} \quad (V-26)$$

Using the I.N.A. values of  $n_i$  and  $B_{n_i}$  (see Appendix B), this method gives for the scalar case

$$\frac{\sigma(0)}{\lambda^2} = 2.69 \times 10^{-5} \quad (\text{V-26a})$$

These two values of  $\frac{\sigma(0)}{\lambda^2}$  differ by a factor of approximately five. This factor of five illustrates that this summation method is very sensitive to the first few values of the parameters,  $n_i$ ,  $m_i$ ,  $B_{n_i}$ , and  $B_{m_i}$ . Therefore, one would expect the "I.N.A. -  $\sigma$ " to be the more accurate one. Examination of Figure V-2 shows that the "small cone angle" evaluation yields  $\frac{\sigma(0)}{\lambda^2} = 3 \times 10^{-5}$  for  $\theta_1 = 15^\circ$ , which is consistent with the I.N.A. results.

The above technique can certainly be applied to other cone angles. However, it would require the detailed computation of the four sets of parameters,  $n_i$ ,  $m_i$ ,  $B_{n_i}$ , and  $B_{m_i}$ . These parameters can be determined by using the technique of Appendix A or by high speed digital computing techniques such as those used by the I.N.A.

An approximation technique for determining  $\sigma(0)$  and  $\sigma'(0)$  appropriate only for small cone angles was discussed in Section V-B. A similar approach can be used for large cone angles.

When this is done (the details are given in Appendix C), the expressions

$$\frac{\sigma'(0)}{\lambda^2} = \frac{1}{16\pi\epsilon^4} [1 - 2\epsilon^2 + \dots] \quad (\text{V-27})$$

and

$$\frac{\sigma(0)}{\lambda^2} = \frac{1}{16\pi\epsilon^4} [1 - 4\epsilon^2 + \dots] \quad (\text{V-28})$$

are obtained, where  $\epsilon = \cos \theta_1$ .

As in the "small cone angle" case, it is interesting to compare these results with the physical optics expression for cross-section, i.e.,

$$\frac{\sigma_{\text{p.o.}}^{(0)}}{\lambda^2} = \frac{\tan^4 \theta_1}{16\pi} = \frac{1}{16\pi \epsilon^4} [1 - 2\epsilon^2 + \epsilon^4] \quad (\text{V-29})$$

The three expressions (V-27), (V-28), and (V-29) are plotted in Figure V-3 for half cone angles between  $50^\circ$  and  $80^\circ$ . No difference between these three evaluations of cross-section can be detected in the range  $80^\circ < \theta_1 < 90^\circ$  when they are displayed graphically using the scale of Figure V-3.

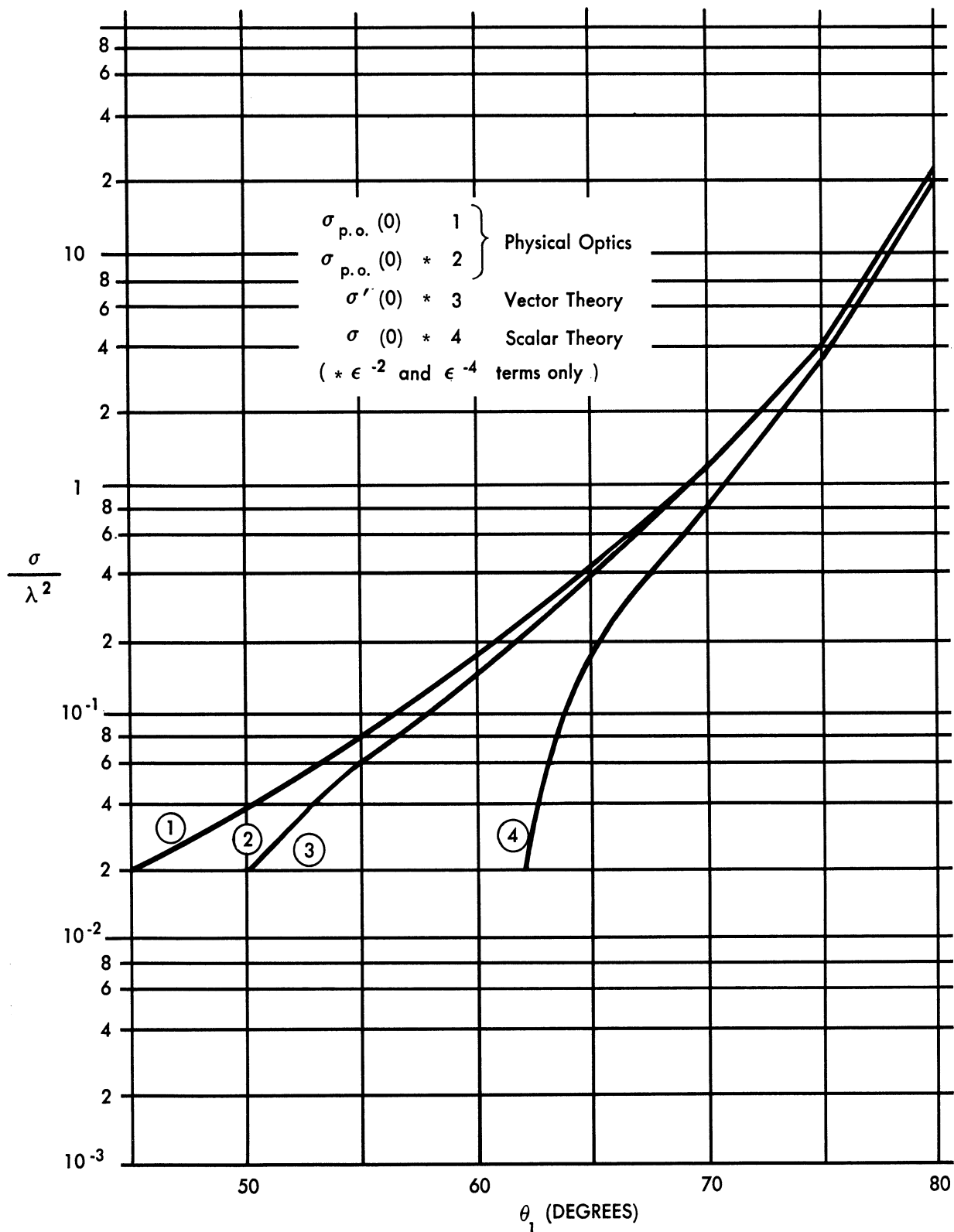


FIG. V - 3 COMPARISON BETWEEN  $\sigma'(0)$ ,  $\sigma(0)$ , AND  $\sigma_{p.o.}(0)$  FOR THE "LARGE CONE ANGLE" APPROXIMATIONS

## VI

CONCLUSION

The exact radar cross-section solution of an infinite cone has been obtained. The excellent agreement between physical optics, exact electromagnetic theory, and experiment is displayed in Figure VI-1.

Examination of Figure VI-1 shows that the theoretical values of  $\sigma'(0)$  and  $\sigma_{p.o.}(0)$  agree with the experimental values for a cone to within a factor of two. In addition these theoretical values are within a factor of three of the experimental ogive data. The comparison between scalar theory and electromagnetic theory is also seen to be good.

If  $\sigma_{p.o.}(0)$  is computed up to the degree of approximation used in finding  $\sigma'(0)$ , there is complete agreement between  $\sigma_{p.o.}(0)$  and  $\sigma'(0)$ . This complete agreement between the approximate determinations of  $\sigma_{p.o.}(0)$  and  $\sigma'(0)$  and their close agreement with the exact value of  $\sigma_{p.o.}(0)$  may imply that the exact value of  $\sigma'(0)$  is identically equal to the physical optics value of  $\sigma_{p.o.}(0) = \frac{\lambda^2 \tan^4 \theta_1}{16\pi}$ .

Outside of the cone problem itself criteria were found in this paper which determine when special summing techniques should be used for scattering problems and when special summing techniques must be used.

It should be emphasized that many more experiments should be made in this field. The amount of experimental information on the cone and other bodies, such as the ogive, the prolate spheroid, and the paraboloid, is very small indeed. It is hoped that more experimenters will enter this field and help fill the gaps in classical electromagnetic theory.

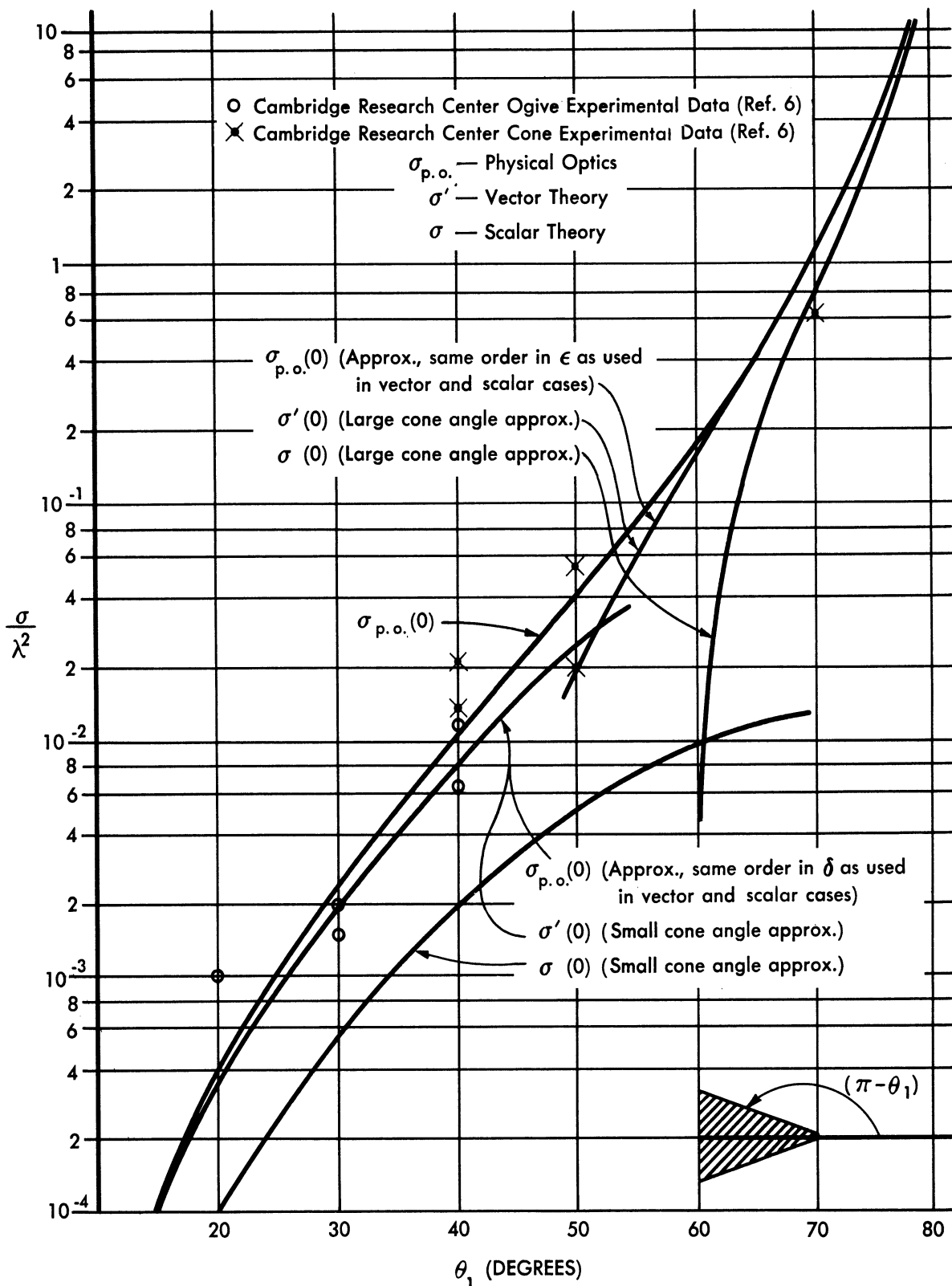


FIG. VI - 1 COMPARISON BETWEEN THEORY AND EXPERIMENT

The authors would like to reiterate the fact that the work of this paper was made possible by the earlier contributions of Spencer, Sletten, Schiff, and Hansen, and by the contribution of unpublished data by Yowell. (See Appendix B).



## APPENDIX A

THE DETERMINATION OF THE QUANTITIES

$$\underline{n_i, m_i, B_{n_i}, \text{ and } B_{m_i}}.^1$$

Since much of the computation involved in this work is based on the values of the Legendre functions,  $P_n(x)$ , the Legendre polynomials for integral values of  $n$  were written out for a greater range in  $n$  than can ordinarily be found in existing literature on this subject. Table A-1 lists the  $P_n(x)$  and  $\frac{dP_n(x)}{dx}$  through  $n = 20$ .

The values of these functions, which appear in Table 3 of Reference 17, were computed from these polynomials using 15-digit accuracy for all intermediate computation. The results were cross-checked to 10-digit accuracy by the use of recursion formulas. The calculations involved in determining the parameters  $n_i$ ,  $m_i$ ,  $B_{n_i}$ , and  $B_{m_i}$  necessitated the computation of other partial derivatives of  $P_y(x)$ . The values of these parameters appear in Reference 17 and Reference 18. The general theory of the approximation methods used is explained in these two references. To illustrate the method of evaluating these parameters in greater detail, we now present all of the formulas that are required to supplement the material of References 17 and 18.

We start with the following definitions:

<sup>1</sup>The material of this appendix was presented, in part, in a talk, "The Zeros of the Legendre function of Order One and Non-Integral Degree", by K. M. Siegel, J. W. Crispin, and R. E. Kleinman, given at the April 25-26, 1952, meeting of the American Mathematical Society held in New York City.

$$N = [n]$$

$$\phi(N, s) = \psi(N + 1 + s) - \psi(N + 1 - s)$$

$$\phi'(N, s) = \psi'(N + 1 + s) - \psi'(N + 1 - s)$$

$$\phi''(N, s) = \psi''(N + 1 + s) - \psi''(N + 1 - s)$$

$$\phi'''(N, s) = \psi'''(N + 1 + s) - \psi'''(N + 1 - s)$$

$$\alpha(N, s, x) = \ln \frac{1+x}{2} + \psi(N + 1 + s) + \psi(N + 1 - s) - 2\psi(s+1)$$

$$\alpha'(N, s) = \psi'(N + 1 + s) + \psi'(N + 1 - s)$$

$$\alpha''(N, s) = \psi''(N + 1 + s) + \psi''(N + 1 - s)$$

$$\alpha'''(N, s) = \psi'''(N + 1 + s) + \psi'''(N + 1 - s)$$

Note: The  $\psi$ -function has the form used in the tables of Reference 19. The argument has been increased by one over that indicated in Reference 17 due to the construction of the tables of Reference 19.

$$A(N, s) = \prod_{r=1}^s (N + 1 - r) \prod_{r=1}^s (N + r) \frac{(-1)^s}{(s!)^2}$$

$$F = \sum_{s=0}^n A(N, s) \alpha(N, s, x) \left( \frac{1+x_0}{2} \right)^s$$

$$F' = \sum_{s=0}^n A(N, s) [\phi(N, s) \alpha(N, s, x) + \alpha'(N, s)] \left( \frac{1+x_0}{2} \right)^s$$

$$F'' = \sum_{s=0}^n A(N, s) \left\{ [\phi(N, s) \alpha(N, s, x) + 2\alpha'(N, s)] \phi(N, s) + \phi'(N, s) \alpha(N, s, x) + \alpha''(N, s) \right\} \left( \frac{1+x_0}{2} \right)^s$$

$$F''' = \sum_{s=0}^n A(N,s) \left\{ [\phi(N,s) a(N,s,x) + 3a'(N,s)] \phi^2(N,s) \right. \\ \left. + 3\phi'(N,s) \phi(N,s) a(N,s,x) + 3\phi'(N,s) a'(N,s) \right. \\ \left. + 3\phi(N,s) a''(N,s) + \phi''(N,s) a(N,s,x) + a'''(N,s) \right\} \left( \frac{1+x_0}{2} \right)^s$$

$$G = \sum_{s=0}^n A(N,s) \left( \frac{1+x_0}{2} \right)^s$$

$$G' = \sum_{s=0}^n A(N,s) \phi(N,s) \left( \frac{1+x_0}{2} \right)^s$$

$$G'' = \sum_{s=0}^n A(N,s) [\phi'(N,s) + \phi^2(N,s)] \left( \frac{1+x_0}{2} \right)^s$$

$$G''' = \sum_{s=0}^n A(N,s) [\phi''(N,s) + 3\phi(N,s) \phi'(N,s) + \phi^3(N,s)] \left( \frac{1+x_0}{2} \right)^s$$

$$\frac{\partial F}{\partial x} = \frac{1}{1+x_0} \left[ \sum \left\{ s(\text{terms in the } \Sigma \text{ for } F) \right\} + G \right]$$

$$\frac{\partial F'}{\partial x} = \frac{1}{1+x_0} \left[ \sum \left\{ s(\text{terms in the } \Sigma \text{ for } F') \right\} + G' \right]$$

$$\frac{\partial F''}{\partial x} = \frac{1}{1+x_0} \left[ \sum \left\{ s(\text{terms in the } \Sigma \text{ for } F'') \right\} + G'' \right]$$

$$\frac{\partial F'''}{\partial x} = \frac{1}{1+x_0} \left[ \sum \left\{ s(\text{terms in the } \Sigma \text{ for } F''') \right\} + G''' \right]$$

$$\frac{\partial G}{\partial x} = \frac{1}{1+x_0} \left[ \sum \left\{ s(\text{terms in the } \Sigma \text{ for } G) \right\} \right]$$

$$\frac{\partial G'}{\partial x} = \frac{1}{1+x_0} \left[ \sum \left\{ s(\text{terms in the } \Sigma \text{ for } G') \right\} \right]$$

$$\frac{\partial G''}{\partial x} = \frac{1}{1+x_0} \left[ \sum \left\{ s(\text{terms in the } \Sigma \text{ for } G'') \right\} \right]$$

$$\frac{\partial G'''}{\partial x} = \frac{1}{1+x_0} \left[ \sum \left\{ s(\text{terms in the } \Sigma \text{ for } G''') \right\} \right]$$

We then have the formulas:

At  $y = N = n = \text{an integer}$

$$\frac{\partial P_y(x)}{\partial y} = (-1)^n [F + G']$$

$$\frac{\partial^2 P_y(x)}{\partial y^2} = (-1)^n [2F' + G'' - \pi^2 G]$$

$$\frac{\partial^3 P_y(x)}{\partial y^3} = (-1)^n [3F'' - \pi^2 F + G''' - 3\pi^2 G']$$

$$\frac{\partial P_y(x)}{\partial x} = (-1)^n \left[ \frac{\partial G}{\partial x} \right]$$

$$\frac{\partial^2 P_y(x)}{\partial x \partial y} = (-1)^n \left[ \frac{\partial F}{\partial x} + \frac{\partial G'}{\partial x} \right]$$

$$\frac{\partial^3 P_y(x)}{\partial x \partial y^2} = (-1)^n \left[ 2 \frac{\partial F'}{\partial x} + \frac{\partial G''}{\partial x} - \pi^2 \frac{\partial G}{\partial x} \right]$$

$$\frac{\partial^4 P_y(x)}{\partial x \partial y^3} = (-1)^n \left[ 3 \frac{\partial F''}{\partial x} - \pi^2 \frac{\partial F}{\partial x} + \frac{\partial G'''}{\partial x} - 3\pi^2 \frac{\partial G'}{\partial x} \right]$$

At  $y = N = n + 1/2$

$$\frac{\partial P_y(x)}{\partial y} = (-1)^n \left[ \frac{F'}{\pi} - \pi G \right]$$

$$\frac{\partial^2 P_y(x)}{\partial y^2} = (-1)^n \left[ \frac{F''}{\pi} - \pi F - 2\pi G' \right]$$

$$\frac{\partial^3 P_y(x)}{\partial y^3} = (-1)^n \left[ \frac{F'''}{\pi} - 3\pi F' - 3\pi G'' + \pi^3 G \right]$$

$$\frac{\partial P_y(x)}{\partial x} = (-1)^n \left[ \frac{1}{\pi} \frac{\partial F}{\partial x} \right]$$

$$\frac{\partial^2 P_y(x)}{\partial x \partial y} = (-1)^n \left[ \frac{1}{\pi} \frac{\partial F'}{\partial x} - \pi \frac{\partial G}{\partial x} \right]$$

$$\frac{\partial^3 P_y(x)}{\partial x \partial y^2} = (-1)^n \left[ \frac{1}{\pi} \frac{\partial F''}{\partial x} - \pi \frac{\partial F}{\partial x} - 2\pi \frac{\partial G'}{\partial x} \right]$$

$$\frac{\partial^4 P_y(x)}{\partial x \partial y^3} = (-1)^n \left[ \frac{1}{\pi} \frac{\partial F'''}{\partial x} - 3\pi \frac{\partial F'}{\partial x} - 3\pi \frac{\partial G''}{\partial x} + \pi^3 \frac{\partial G}{\partial x} \right]$$

The values of  $P_y(x)$  and its derivatives are given in Table A-2 for  $x_0 = \cos 165^\circ$ . Values of  $P_y(x)$  and  $\frac{\partial P_y(x)}{\partial x}$  are included for completeness. As mentioned above, 10 place values for these quantities appear in Table 3 of Reference 17.

In Reference 18, the values of  $\int_{x_0}^1 [P_{m_i}^1(x)]^2 dx$  were tabulated as computed without using  $\left. \frac{\partial^3 P_y(x)}{\partial y^3} \right|_{\substack{x=x_0 \\ y=N}}$  and  $\left. \frac{\partial^4 P_y(x)}{\partial x \partial y^3} \right|_{\substack{x=x_0 \\ y=N}}$

Also the values of some of these integrals were shown as re-evaluated to include the extra derivatives. Similarly in Table 4

of Reference 17 the values of  $\int_{x_0}^1 [P_{n_i}(x)]^2 dx$  were given as

evaluated without using the two derivatives mentioned above. We show in Table A-3 those values of both sets of integrals, as re-evaluated by using the extra derivatives, which were not included in the tables of References 17 and 18.

In order to illustrate further the effect of including  $\left. \frac{\partial^3 P_y(x)}{\partial y^3} \right|_{\substack{x=x_0 \\ y=N}}$  and  $\left. \frac{\partial^4 P_y(x)}{\partial x \partial y^3} \right|_{\substack{x=x_0 \\ y=N}}$  in the evaluation of the two sets of integrals, we show three charts. In Chart A-I, we show the graph of  $\int_{x_0}^1 [P_{n_i}(x)]^2 dx$

as based on the "best" values as explained in Reference 17. Also shown are the corresponding values as re-computed by using the extra derivatives. Chart A-II gives a similar representation of

$\frac{1}{m_i(m_i + 1)} \int_{x_0}^1 [P_{m_i}^1(x)]^2 dx$ . Note that in both cases the new

points lie on a much smoother curve which is very nearly an envelope of the set of discontinuous curves originally plotted. The smoothness of these new curves seems to indicate that there would be no appreciable increase in accuracy if still more derivatives were used. Chart A-III shows the new points from Charts A-I and A-II on a single graph.

Reference 20 shows how the  $n_i$  can be evaluated to any desired degree of accuracy by the use of hypergeometric series, although the labor involved is far greater than that needed for the approximation method used here. Similarly the  $m_i$  can be computed much more accurately by use of the same technique. The procedures outlined in the Appendix of Reference 20 can also be employed for the  $m_i$  computation by including the factor  $\frac{1+k(1+\mu)}{1+(k-1)(1+\mu)}$ , where  $x = \frac{1-\mu}{2}$ , in  $\frac{A_k}{A_{k-1}}$ .

TABLE A-1

## LEGENDRE POLYNOMIALS

$$P_0(x) = 1$$

$$P_1(x) = x$$

$$P_2(x) = \frac{1}{2} (3x^2 - 1)$$

$$P_3(x) = \frac{x}{2} (5x^2 - 3)$$

$$P_4(x) = \frac{1}{8} (35x^4 - 30x^2 + 3)$$

$$P_5(x) = \frac{x}{8} (63x^4 - 70x^2 + 15)$$

$$P_6(x) = \frac{1}{16} (231x^6 - 315x^4 + 105x^2 - 5)$$

$$P_7(x) = \frac{x}{16} (429x^6 - 693x^4 + 315x^2 - 35)$$

$$P_8(x) = \frac{1}{128} (6435x^8 - 12012x^6 + 6930x^4 - 1260x^2 + 35)$$

$$P_9(x) = \frac{x}{128} (12155x^8 - 25740x^6 + 18018x^4 - 4620x^2 + 315)$$

$$P_{10}(x) = \frac{1}{256} (46189x^{10} - 109395x^8 + 90090x^6 - 30030x^4 + 3465x^2 - 63)$$

TABLE A-1 (Continued)

$$P_{11}(x) = \frac{x}{256} (88179x^{10} - 230945x^8 + 218790x^6 - 90090x^4 + 15015x^2 - 693)$$

$$P_{12}(x) = \frac{1}{1024} (676039x^{12} - 1939938x^{10} + 2078505x^8 - 1021020x^6 + 225225x^4 - 18018x^2 + 231)$$

$$P_{13}(x) = \frac{x}{1024} (1300075x^{12} - 4056234x^{10} + 4849845x^8 - 2771340x^6 + 765765x^4 - 90090x^2 + 3003)$$

$$P_{14}(x) = \frac{1}{2048} (5014575x^{14} - 16900975x^{12} + 22309287x^{10} - 14549535x^8 + 4849845x^6 - 765765x^4 + 45045x^2 - 429)$$

$$P_{15}(x) = \frac{x}{2048} (9694845x^{14} - 35102025x^{12} + 50702925x^{10} - 37182145x^8 + 14549535x^6 - 2909907x^4 + 255255x^2 - 6435)$$

$$P_{16}(x) = \frac{1}{32768} (300540195x^{16} - 1163381400x^{14} + 1825305300x^{12} - 1487285800x^{10} + 669278610x^8 - 162954792x^6 + 19399380x^4 - 875160x^2 + 6435)$$

$$P_{17}(x) = \frac{x}{32768} (583401555x^{16} - 2404321560x^{14} + 4071834900x^{12} - 3650610600x^{10} + 1859107250x^8 - 535422888x^6 + 81477396x^4 - 5542680x^2 + 109395)$$

$$P_{18}(x) = \frac{1}{65536} (2268783825x^{18} - 9917826435x^{16} + 18032411700x^{14} - 17644617900x^{12} + 10039179150x^{10} - 3346393050x^8 + 624660036x^6 - 58198140x^4 + 2078505x^2 - 12155)$$



TABLE A-1 (Continued)

$$P_{19}(x) = \frac{x}{65536} (4418157975x^{18} - 20419054425x^{16} + 39671305740x^{14} \\ - 42075627300x^{12} + 26466926850x^{10} - 10039179150x^8 \\ + 2230928700x^6 - 267711444x^4 + 14549535x^2 - 230945)$$

$$P_{20}(x) = \frac{1}{262144} (34461632205x^{20} - 167890003050x^{18} + 347123925225x^{16} \\ - 396713057400x^{14} + 273491577450x^{12} - 116454478140x^{10} \\ + 30117537450x^8 - 4461857400x^6 + 334639305x^4 \\ - 9699690x^2 + 46189)$$

TABLE A-1a

DERIVATIVES (with respect to x) OF THE  
LEGENDRE POLYNOMIALS

$$P_0'(x) = 0$$

$$P_1'(x) = 1$$

$$P_2'(x) = 3x$$

$$P_3'(x) = \frac{3}{2} (5x^2 - 1)$$

$$P_4'(x) = \frac{5x}{2} (7x^2 - 3)$$

$$P_5'(x) = \frac{15}{8} (21x^4 - 14x^2 + 1)$$

$$P_6'(x) = \frac{21x}{8} (33x^4 - 30x^2 + 5)$$

$$P_7'(x) = \frac{7}{16} (429x^6 - 495x^4 + 135x^2 - 5)$$

$$P_8'(x) = \frac{9x}{16} (715x^6 - 1001x^4 + 385x^2 - 35)$$

TABLE A-1a (Continued)

$$P'_9(x) = \frac{45}{128} (2431x^8 - 4004x^6 + 2002x^4 - 308x^2 + 7)$$

$$P'_{10}(x) = \frac{55x}{128} (4199x^8 - 7956x^6 + 4914x^4 - 1092x^2 + 63)$$

$$P'_{11}(x) = \frac{33}{256} (29393x^{10} - 62985x^8 + 46410x^6 - 13650x^4 + 1365x^2 - 21)$$

$$P'_{12}(x) = \frac{39x}{256} (52003x^{10} - 124355x^8 + 106590x^6 - 39270x^4 + 5775x^2 - 231)$$

$$P'_{13}(x) = \frac{91}{1024} (185725x^{12} - 490314x^{10} + 479655x^8 - 213180x^6 + 42075x^4 - 2970x^2 + 33)$$

$$P'_{14}(x) = \frac{35x}{1024} (1002915x^{12} - 2897310x^{10} + 3187041x^8 - 1662804x^6 + 415701x^4 - 43758x^2 + 1287)$$

$$P'_{15}(x) = \frac{15}{2048} (9694845x^{14} - 30421755x^{12} + 37182145x^{10} - 22309287x^8 + 6789783x^6 - 969969x^4 + 51051x^2 - 429)$$

$$P'_{16}(x) = \frac{17x}{2048} (17678835x^{14} - 59879925x^{12} + 80528175x^{10} - 54679625x^8 + 19684665x^6 - 3594591x^4 + 285285x^2 - 6435)$$

$$P'_{17}(x) = \frac{153}{32768} (64822395x^{16} - 235717800x^{14} + 345972900x^{12} - 262462200x^{10} + 109359250x^8 - 24496472x^6 + 2662660x^4 - 108680x^2 + 715)$$

$$P'_{18}(x) = \frac{171x}{32768} (119409675x^{16} - 463991880x^{14} + 738168900x^{12} - 619109400x^{10} + 293543250x^8 - 78278200x^6 + 10958948x^4 - 680680x^2 + 12155)$$

TABLE A-1a (Continued)

$$P'_{19}(x) = \frac{95}{65536} (883631595x^{18} - 3653936055x^{16} + 6263890380x^{14} \\ - 5757717420x^{12} + 3064591530x^{10} - 951080130x^8 \\ + 164384220x^6 - 14090076x^4 + 459459x^2 - 2431)$$

$$P'_{20}(x) = \frac{105x}{65536} (1641030105x^{18} - 7195285845x^{16} + 13223768580x^{14} \\ - 13223768580x^{12} + 7814045070x^{10} - 2772725670x^8 \\ + 573667380x^6 - 63740820x^4 + 3187041x^2 - 46189)$$

TABLE A-2

VALUES OF LEGENDRE FUNCTIONS AND DERIVATIVES FOR  $x = \cos 165^\circ$  AND  $y = i$

i	$P_y(x)$	$\frac{\partial P_y(x)}{\partial x}$	$\frac{\partial P_y(x)}{\partial y}$	$\frac{\partial^2 P_y(x)}{\partial x \partial y}$	$\frac{\partial^2 P_y(x)}{\partial y^2}$	$\frac{\partial^3 P_y(x)}{\partial x \partial y^2}$	$\frac{\partial^3 P_y(x)}{\partial y^3}$	$\frac{\partial^4 P_y(x)}{\partial x \partial y^3}$
1.	-.96593	+ 1.0000	+1.96767	-31.4201	+6.65926	- 15.5070	-18.1077	+280.4622
1.5	+.40531	-10.9463	+2.57248	- 6.90411	-4.27345	+ 96.1650	-18.57077	+ 79.0258
2.	+.89952	- 2.8978	- .83151	+33.3189	-6.99490	+ 31.9902	+ 8.85285	-288.6843
2.5	-.09820	+11.5866	-2.42716	+13.2839	+1.49086	- 98.6800	+19.11724	-132.6410
3.	-.80416	+ 5.4976	+ .03762	-33.7786	+6.55209	- 53.5628	- 1.90483	+284.3069
3.5	-.12691	-11.5354	+2.15301	-21.4427	+ .55693	+ 95.6504	-17.63258	+199.7114
4.	+.68470	- 8.5269	+ .55236	+31.9740	-5.72620	+ 78.0203	- 3.37350	-262.5904
4.5	+.29430	+10.5713	-1.79864	+30.2723	-2.08678	- 85.5819	+15.09171	-270.5686
5.	-.54713	+11.6599	- .98476	-27.4380	+4.66630	-102.8882	+ 7.29546	+219.5962
5.5	-.41302	- 8.5925	+1.39206	-38.8391	+3.18357	+ 67.5910	-11.91910	+338.0942
6.	+.39831	-14.5453	+1.27923	+20.0474	-3.46794	+125.4107	-10.01824	-154.3421
6.5	+.48750	+ 5.6150	- .95798	+46.1510	-3.89064	- 41.8106	+ 8.40506	-394.4973
7.	-.24554	+16.8378	-1.44737	-10.0114	+2.21014	-142.8545	+11.64229	+ 68.55149
7.5	-.52104	- 1.7674	+ .51982	-51.2758	+4.23964	+ 9.2902	- 4.78779	+432.4211
8.	+.09618	-18.2284	+1.49951	- 2.1543	- .96401	+152.7732	-12.25865	+ 33.55306
8.5	+.51722	- 2.7217	- .09965	+53.4261	-4.26309	+ 28.1030	+ 1.27606	-445.6640
9.	+.04277	+18.4730	-1.44745	+15.6726	- .20615	-153.2447	+11.97032	-145.6297
9.5	-.48040	+ 7.5425	- .28249	-52.0351	+3.99940	- 67.8441	+ 1.94733	+427.8117
10.	-.16506	-17.4158	+1.30552	-29.5703	+1.24419	+143.0667		
10.5	+.41592	-12.3297	+ .60942	+46.8156	-3.49440	+106.9611	- 4.72841	-382.7211
11.	+.26549	+15.0068	-1.09060	+42.7584	-2.10402	-121.8947		
11.5	-.32922	+16.6926	- .86760	-37.7962	+2.80080	-142.2833	+ 6.94652	+304.8202
12.	-.34022	-11.3096	+ .82173	-54.1232	+2.75140	+ 90.3117		
12.5	+.22922	-20.2478	+1.04774	+25.3334	-1.97642	-170.7213	- 8.51829	-199.1999
13.	+.38690	+ 6.5014	- .51933	+62.6213	-3.16523	- 49.8228		
13.5	-.12094	+22.6524	-1.14518	-10.0965	+1.08174	-189.4793	+ 9.40032	+ 71.48611
14.	-.40482	- .8633	+ .20422	-67.3711	+3.33825	+ 2.7733		
14.5	+.01217	-23.6343	+1.16002	- 6.9736	- .17695	+196.4178	- 9.58984	+ 70.49965
15.	+.39489	- 5.2385	+ .10335	+67.7340	-3.27697	+ 47.8035		
15.5	+.09038	+23.0176	-1.09695	+24.7285	- .68099	-190.1477	+ 9.12328	-217.2708
16.	-.35950	+11.3782	- .38478	-63.3776	+3.00079	- 98.3994		
16.5	-.18075	-20.7420	+ .96484	-41.8952	+1.44124	+170.2384	- 8.07277	+358.3586
17.	+.30241	-17.1019	+ .62404	+54.3173	-2.54050	+145.2905		
17.5	+.25399	+16.8721	- .77613	+57.1716	-2.06158	-137.2863		

TABLE A-3

VALUES OF  $\int_{x_0}^1 [P_{n_i}(x)]^2 dx$ , USING  $\left. \frac{\partial^3 P_y(x)}{\partial y^3} \right|_{x=x_0, y=n_i}$  AND  $\left. \frac{\partial^4 P_y(x)}{\partial x \partial y^3} \right|_{x=x_0, y=n_i}$   $x_0 = \cos 165^\circ$

$n_i = j + z'_j$	$\int_{x_0}^1 [P_{n_i}(x)]^2 dx$	$n_i(n_i+1) \int_{x_0}^1 [P_{n_i}(x)]^2 dx$	$n_i = j + \frac{1}{2} + z''_j$	$\int_{x_0}^1 [P_{n_i}(x)]^2 dx$	$n_i(n_i+1) \int_{x_0}^1 [P_{n_i}(x)]^2 dx$
1.03158	.625683	1.31127			
2.08361	.365737	2.34988			
3.14588	.258622	3.37306			
4.21990	.202284	4.44054	4.24367	.197114	4.38625
			5.31014	.159313	5.33822
			6.38439	.134097	6.32199
			7.46564	.115786	7.31785
			8.55028	.101809	8.31348
			9.63336	.091175	9.33955
			10.71202	.083506	10.47667

VALUES OF  $\int_{x_0}^1 [P^1_{m_i}(x)]^2 dx$ , USING  $\left. \frac{\partial^3 P_y(x)}{\partial y^3} \right|_{x=x_0, y=m_i}$  AND  $\left. \frac{\partial^4 P_y(x)}{\partial x \partial y^3} \right|_{x=x_0, y=m_i}$   $x_0 = \cos 165^\circ$

$m_i = j + z'_j$	$\int_{x_0}^1 [P^1_{m_i}(x)]^2 dx$	$\frac{1}{m_i(m_i+1)} \int_{x_0}^1 [P^1_{m_i}(x)]^2 dx$	$m_i = j + \frac{1}{2} + z''_j$	$\int_{x_0}^1 [P^1_{m_i}(x)]^2 dx$	$\frac{1}{m_i(m_i+1)} \int_{x_0}^1 [P^1_{m_i}(x)]^2 dx$
0.9673	1.35806	.71365			
1.9198	2.42491	.43260			
2.8894	3.37945	.30072			
3.8900	4.28564	.22530			
4.9180	5.18033	.17799			
5.9657	6.09038	.14656			
7.0264	7.03236	.12469			
8.0940	7.93860	.10785			
9.1638	8.66236	.093005			
			10.248	10.0889	.087524
			11.333	11.5397	.082562
			12.410	12.0322	.072301
			13.492	12.8305	.065620
			14.576	13.7103	.060388
			15.658	14.1082	.054089
			16.750	16.8298	.056606

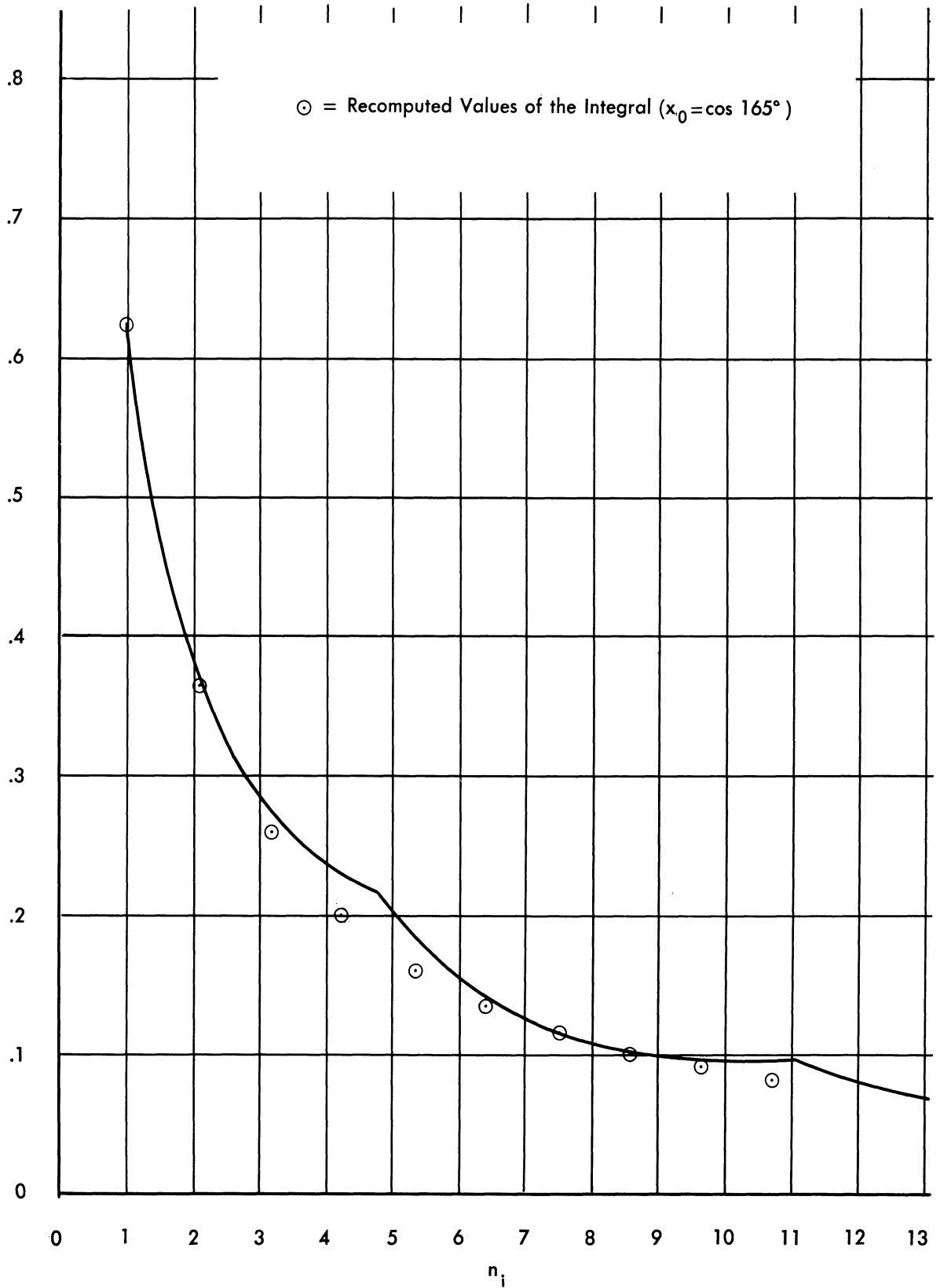


CHART A-1 GRAPH REPRESENTING "BEST VALUES" OF  $\int_{x_0}^1 [P_{n_i}(x)]^2 dx$  vs.  $n_i$   
 AS ORIGINALLY COMPUTED

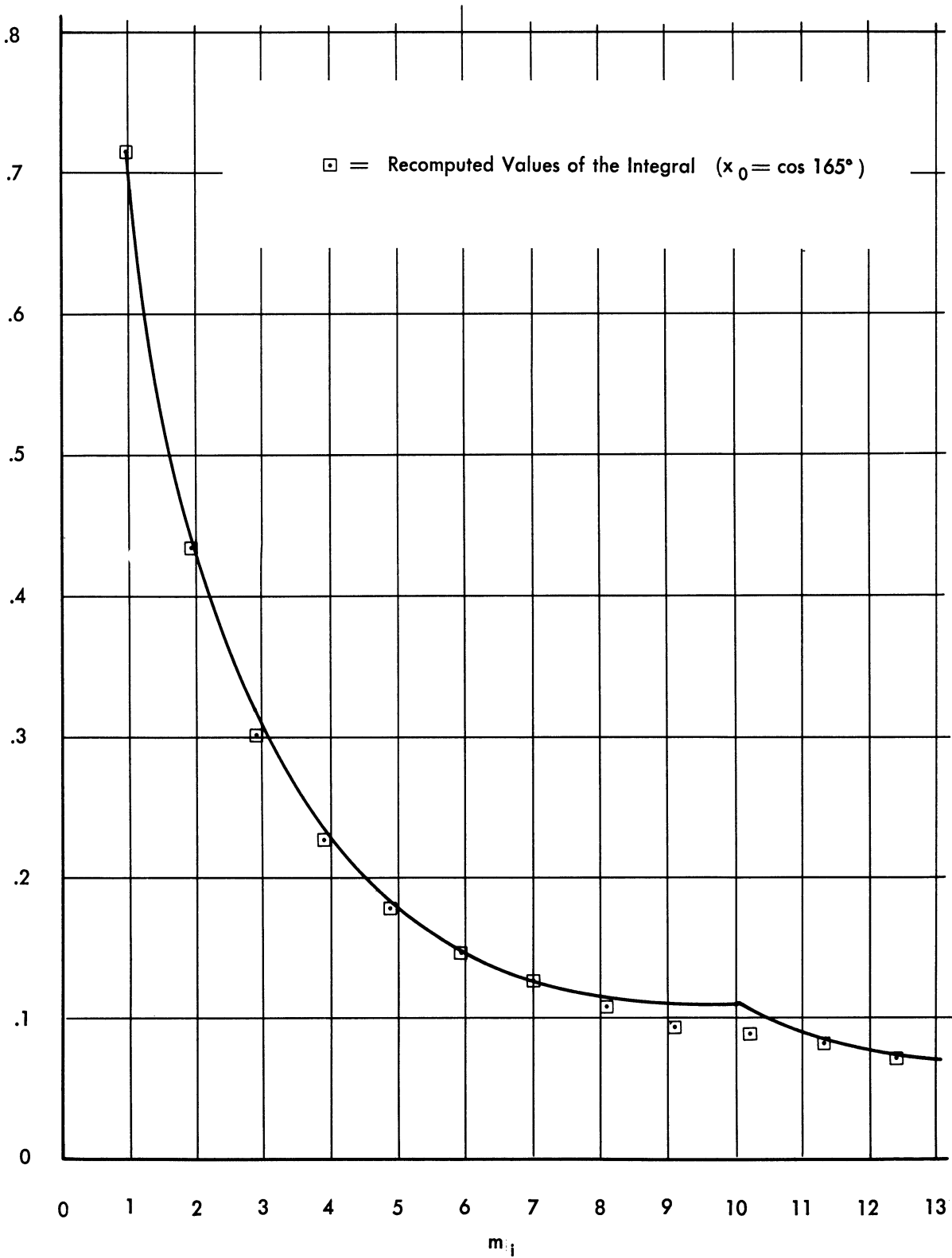


CHART A-II GRAPH REPRESENTING "BEST VALUES" OF  $\frac{1}{m_i(m_i+1)} \int_{x_0}^1 [P_{m_i}^1(x)]^2 dx$  vs.  $m_i$  AS ORIGINALLY COMPUTED

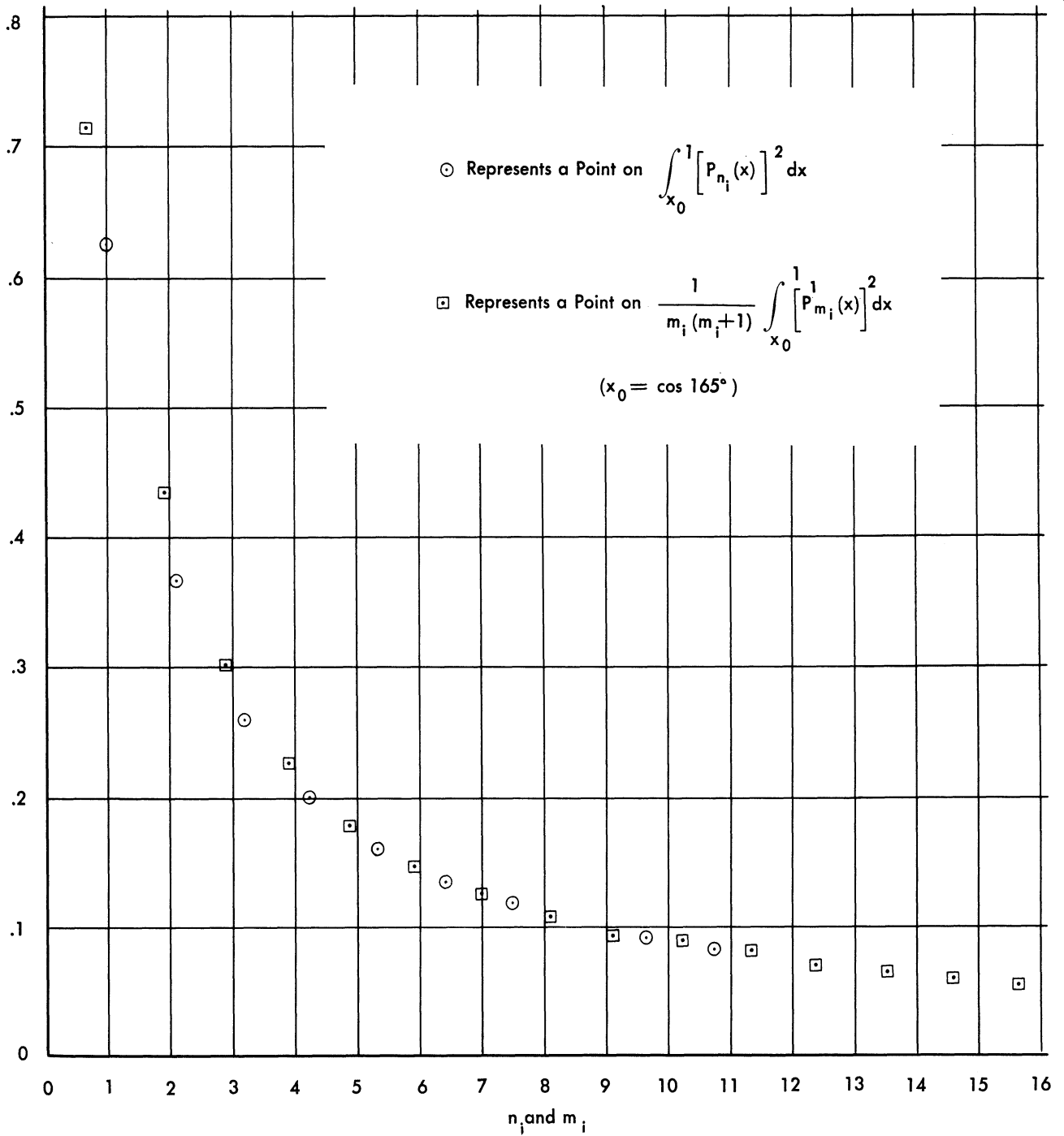


CHART A-III GRAPH REPRESENTING "BEST VALUES" OF  $\int_{x_0}^1 [P_{n_i}(x)]^2 dx$  AND  $\frac{1}{m_i(m_i+1)} \int_{x_0}^1 [P_{m_i}^1(x)]^2 dx$  AS RECOMPUTED USING  $\frac{\partial^3 P_y(x)}{\partial y^3} \Big|_{x=x_0, y=n_i \text{ or } m_i}$  AND  $\frac{\partial^4 P_y(x)}{\partial x \partial y^3} \Big|_{x=x_0, y=n_i \text{ or } m_i}$



## APPENDIX B

CERTAIN VALUES OF  $n_i$  AND  $B_{n_i}$  COMPUTED BY THE I.N.A.

The Institute of Numerical Analysis at the University of California at Los Angeles has computed the parameters  $n_i$  and  $B_{n_i}$  for  $\theta_0 = 165^\circ$ . Those values computed by the I.N.A. that are employed in this report in computing  $\sigma(0)$  are listed below. The authors would like to express their appreciation and gratitude to Dr. Everett Yowell and the I.N.A. for their cooperation in furnishing these unpublished data, thereby making the computation of  $\sigma(0)$  for  $\theta_0 = 165^\circ$  possible.

$i$	$n_i$	$B_{n_i}$
1	1.03163	1.31078
2	2.08443	2.34637
3	3.14992	3.34731
4	4.22309	4.34068
5	5.30108	5.33248
6	6.38224	6.32443
7	7.46557	7.31653

## APPENDIX C

DERIVATION OF SCALAR AND VECTOR CROSS-SECTIONS  
IN THE LARGE CONE ANGLE CASE

When  $\theta_1$  is close to  $\pi/2$ ,  $\cos(\pi - \theta_1) = -\cos \theta_1 = -\epsilon$ . Thus we may write

$$P_{\eta}^1(-\epsilon) = \frac{2 \cos\left(\frac{\eta+1}{2}\pi\right) \Gamma\left(\frac{\eta+2}{2}\right)}{\Gamma\left(\frac{\eta+1}{2}\right) \sqrt{\pi}} \sqrt{1-\epsilon^2}$$

$$\times \left[ 1 + \frac{\left(\frac{\eta+2}{2}\right)\left(\frac{1-\eta}{2}\right)}{\frac{1}{2}} \epsilon^2 + \frac{\left(\frac{\eta+2}{2}\right)\left(\frac{\eta+4}{2}\right)\left(\frac{1-\eta}{2}\right)\left(\frac{3-\eta}{2}\right)}{\frac{1}{2} \cdot \frac{3}{2} \cdot 2} \epsilon^4 + \dots \right]$$

$$- \frac{4 \sin\left(\frac{\eta+1}{2}\pi\right) \Gamma\left(\frac{\eta+3}{2}\right)}{\Gamma\left(\frac{\eta}{2}\right) \sqrt{\pi}} \epsilon \sqrt{1-\epsilon^2}$$

$$\times \left[ 1 + \frac{\left(\frac{\eta+3}{2}\right)\left(\frac{2-\eta}{2}\right)}{\frac{3}{2}} \epsilon^2 + \frac{\left(\frac{\eta+3}{2}\right)\left(\frac{\eta+5}{2}\right)\left(\frac{2-\eta}{2}\right)\left(\frac{4-\eta}{2}\right)}{\frac{3}{2} \cdot \frac{5}{2} \cdot 2} \epsilon^4 + \dots \right]$$

Using this expression of the Legendre function and the definitions of the two quantities  $n_i$  and  $m_i$ , we obtain

$$n_i = 2i - \frac{2i}{\pi} (2i+1) \beta_i^2 \epsilon + \frac{2i^2 (2i+1)^2}{\pi^2} \left\{ \frac{1}{i} + \frac{1}{i+\frac{1}{2}} - 4\alpha_{2i}^{(1)} \right\} \beta_i^4 \epsilon^2 + \dots$$

$$m_i = 2i - 1 - 4A_1 \epsilon - 8 \left[ A_1^2 A_2 - A_1 A_3 \right] \epsilon^2 + \dots$$

where

$$\alpha_i^{(m)} \equiv \sum_{\eta=i+1}^{\infty} \frac{(-1)^{\eta+1}}{\eta^m} \left\{ \alpha_{2i}^{(1)} \approx \frac{1}{4i} \right\}^1$$

$$\beta_i = \frac{\Gamma(i + 1/2)}{\Gamma(i + 1)} \approx \frac{1}{\sqrt{i}}^1$$

$$A_1 = A_0 \left[ -\frac{1}{2} - 2(i - 1) \left( i + \frac{1}{2} \right) \right] \div A_0'$$

$$A_2 = \frac{1}{i - 1/2} + 2\alpha_{2i}^{(1)}$$

$$A_3 = \left[ \frac{A_0'' A_0' A_1}{A_0} - 4A_0 (i - 1/4) \right] \div A_0'$$

with

$$A_0 = (-1)^i \frac{2i \beta_i}{\sqrt{\pi}} \qquad A_0' = (-1)^{i+1} \frac{4\sqrt{\pi}}{\beta_i} (i - 1/2)$$

$$A_0'' = A_0 \left\{ \frac{1}{i} - 2\alpha_{2i}^{(1)} \right\}$$

In order to obtain  $\sigma'(0)$  and  $\sigma(0)$  [Equations (V-27) and (V-28)], it is necessary, as in the small angle case, to find the sums of a number of series. The basic formula for finding these sums is

$$\sum_{i=1}^{\infty} V_i = \frac{(1 - 2x) V_1 + V_2 + \sum_{i=1}^{\infty} \left\{ V_{i+2} - 2x V_{i+1} + x^2 V_i \right\}}{(1 - x)^2}$$

with  $x = \exp \left\{ \frac{\pi^2 j}{\pi - \theta_1} \right\}$  and  $\theta_1 = \frac{1}{2}$  cone angle.

<sup>1</sup>The asymptotic forms hold for  $i \gg 1$ .

For the  $n_i$  series  $V_i = \frac{n_i(n_i + 1) e^{\pi n_i j}}{B_{n_i}}$ . By using the ex-

pression given for  $n_i$ ,  $V_i$  can be expressed in the form

$V_i = (V_i^{(0)} + V_i^{(1)} \epsilon + V_i^{(2)} \epsilon^2 + \dots)$ .  $x = \exp\left\{\frac{\pi^2 j}{\pi - \theta_1}\right\}$  can also be expressed as a series in  $\epsilon$  as follows:

$$x = 1 - 4j\epsilon - 8\left(1 - \frac{j}{\pi}\right) \epsilon^2 + \left(10j - \frac{16j}{\pi^2} + \frac{32}{\pi}\right) \epsilon^3 + \dots$$

Using these series and the fact that  $V_n^{(0)} = 4n + 1$  it can be shown that

$$\begin{aligned} & (1 - 2x) V_1 + V_2 + \sum_{i=1}^{\infty} (V_{i+2} - 2x V_{i+1} + x^2 V_i) \\ &= \lim_{i \rightarrow \infty} \left\{ (V_{i+1}^{(0)} - V_i^{(0)}) + \left[ (V_{i+1}^{(1)} - V_i^{(1)}) + 8j V_i^{(0)} \right] \epsilon \right. \\ & \left. + \left[ (V_{i+1}^{(2)} - V_i^{(2)}) + 16 \left(1 - \frac{j}{\pi}\right) V_i^{(0)} + 8j V_i^{(1)} - 16(2i^2 - i) + 16 \right] \epsilon^2 + \dots \right\} \end{aligned}$$

Upon applying these series, we find that

$$\sum_{i=1} \frac{n_i(n_i + 1) e^{\pi n_i j}}{B_{n_i}} = -\frac{1}{4\epsilon^2} \left[ 1 + 2\epsilon^2 + \dots \right].$$

The  $m_i$  series can be evaluated in the same way. The final expressions for cross-section are given in the text in Section V-C.

APPENDIX D

DERIVATION OF AN INTEGRAL EXPRESSION  
FOR THE SUM OCCURRING IN  $\sigma'(0)$

$\sigma'(0)$  is given by Equation (V-19) as

$$\sigma'(0) = \frac{\lambda^2}{4\pi} \left| \sum_i \left\{ \frac{n_i(n_i + 1)}{B_{n_i}} e^{j\pi n_i} - \frac{m_i(m_i + 1)}{B_{m_i}} e^{j\pi m_i} \right\} \right|^2 \quad (V-19)$$

As noted before, one must apply a summation technique to this sum since it is divergent as it stands. In this appendix the sum will be defined as follows:

$$\sigma'(0) = \lim_{\alpha \rightarrow 0} \frac{\lambda^2}{4\pi} \times \left| \sum_{i=1} \left\{ \frac{n_i(n_i + 1)}{B_{n_i}} e^{j\pi n_i - \alpha \left( n_i + \frac{1}{2} \right)} - \frac{m_i(m_i + 1)}{B_{m_i}} e^{j\pi m_i - \alpha \left( m_i + \frac{1}{2} \right)} \right\} \right|^2 \quad (D-1)$$

It is shown that this summation method always yields the same answer as the summation method used elsewhere in this paper whenever the latter method gives a finite result. Using the definitions of  $B_{n_i}$  and  $B_{m_i}$  as given in UMM-87 we find that Equation (D-1) becomes

$$\sigma'(0) = \lim_{\alpha \rightarrow 0} \frac{\lambda^2}{4\pi} \left| \sum_{i=1}^{\infty} \left\{ \frac{n_i(n_i + 1)(2n_i + 1) \exp \left[ j\pi n_i - \alpha \left( n_i + \frac{1}{2} \right) \right]}{(\mu_o^2 - 1) \frac{dP_{n_i}^1(\mu_o)}{d\mu} \frac{dP_{n_i}^1(\mu_o)}{dn_i}} \right. \right. \\ \left. \left. + \frac{m_i(m_i + 1)(2m_i + 1) \exp \left[ j\pi m_i - \alpha \left( m_i + \frac{1}{2} \right) \right]}{(\mu_o^2 - 1) \frac{d^2 P_{m_i}^1(\mu_o)}{d\mu dm_i} P_{m_i}^1(\mu_o)} \right\} \right|^2 \quad (D-2)$$

Representing the sum on the right by  $S_\alpha$  (D-2) takes on the form

$$\sigma'(0) = \lim_{\alpha \rightarrow 0} \frac{\lambda^2}{4\pi} \left| S_\alpha \right|^2 = \frac{\lambda^2}{4\pi} \left| \lim_{\alpha \rightarrow 0} S_\alpha \right|^2 = \frac{\lambda^2}{4\pi} \left| S_o \right|^2 \quad (D-3)$$

Now the  $n_i$  and  $m_i$  are given by  $P_{n_i}^1(\mu_o) = 0 = \frac{dP_{n_i}^1(\mu_o)}{d\mu} \left( n_i, m_i > -\frac{1}{2} \right)$ .

Thus, the  $n_i$  and  $m_i$  are all distinct except for  $n_o = m_o = 0$ .

Furthermore, the  $n_i$  and  $m_i$  are all real (Ref. 21). Thus,  $S_\alpha$  is the sum of the residues of the function

$$f_\alpha(z) = \frac{z(z + 1)(2z + 1) \exp \left[ j\pi z - \alpha \left( z + \frac{1}{2} \right) \right]}{(\mu_o^2 - 1) \frac{dP^1(\mu_o)}{d\mu} \frac{z}{z} P_z^1(\mu_o)} \quad (D-4)$$

at the poles of the function where  $\text{Re}(z) > 0$ . Thus, if  $C_R$  is the contour shown in Figure D-1,  $S_\alpha$  is given by

$$S_\alpha = - \left. \frac{e^{-\alpha/2} (\mu_o^2 - 1)^{-1}}{\frac{dP^1(\mu_o)}{z} \frac{dP^1(\mu_o)}{z}} \right|_{z=0} + \lim_{R \rightarrow \infty} \frac{1}{2\pi j} \int_{C_R} f_\alpha(z) dz, \quad (D-5)$$

where account has been taken of the pole at  $z = 0$ . Making use of the relation

UMM-92

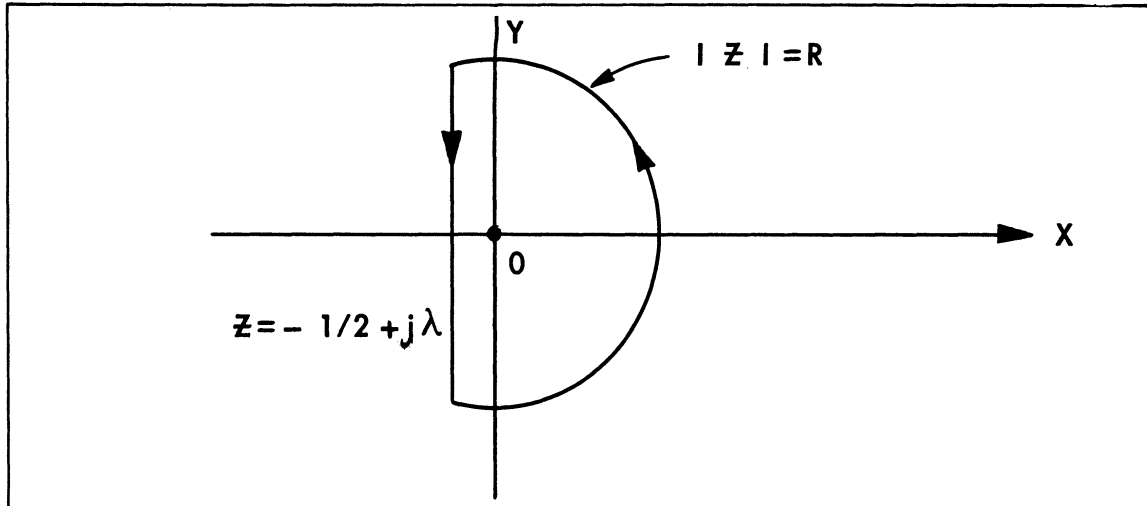


FIG. D-1

$$\left. \frac{dP_z(\mu_0)}{dz} \right|_{z=z_0} = \ln \frac{1 + \mu_0}{2}$$

(Ref. 14, p. 76), the first term on the right of Equation (D-5) becomes

$$-\frac{1 + \mu_0}{1 - \mu_0} e^{-a/2}.$$

By making use of asymptotic relations it can be shown that for large  $|z|$

$$f_a(z) \approx \frac{2\pi z \sin^2 \theta_0 \exp \left[ j\pi z - a \left( z + \frac{1}{2} \right) \right]}{\cos \left[ (2z + 1) \theta_0 \right]} \quad (D-6)$$

Near the positive real axis the factor  $e^{-az}$  makes (D-6) go to zero exponentially with R. Since  $\theta_0 > \pi/2$ , the factor

$\frac{e^{j\pi z}}{\cos \left[ (2z + 1) \theta_0 \right]}$  goes to zero exponentially with R except near the real axis. Thus, on the entire circular arc of  $C_R$ ,  $f_a(z)$  goes to zero exponentially with R and the integral around the arc vanishes in the limit  $R \rightarrow \infty$ . As a result Equation (D-5) can be written in the form

$$\begin{aligned}
 S_a &= - \left( \frac{1 + \mu_o}{1 - \mu_o} \right) e^{-a/2} \\
 &+ \frac{1}{2\pi j} \int_{-\infty}^{\infty} \frac{\left(-\frac{1}{2} + jS\right)\left(\frac{1}{2} + jS\right) (2jS) \exp \left[ -\frac{1}{2} \pi j - \pi S - jaS \right]}{(\mu_o^2 - 1) \frac{1}{2} \frac{d}{d\mu} \left[ K_S^1(\mu_o) \right]^2} (-jdS) \\
 &= - \frac{1 + \mu_o}{1 - \mu_o} e^{-a/2} + \frac{1}{2\pi} \int_{-\infty}^{\infty} \frac{S(4S^2 + 1) \exp \left[ -\pi S - jaS \right]}{(\mu_o^2 - 1) \frac{d}{d\mu} \left[ K_S^1(\mu_o) \right]^2} dS
 \end{aligned} \tag{D-7}$$

where

$$K_S^m(\mu) \equiv P_{-\frac{1}{2} + jS}^m(\mu) .$$

Since the integral on the right of (D-7) is uniformly convergent it follows that

$$S_o = \lim_{a \rightarrow 0} S_a = - \frac{1 + \mu_o}{1 - \mu_o} - \frac{1}{2\pi} \int_{-\infty}^{\infty} \frac{S (4S^2 + 1) e^{-\pi S}}{(1 - \mu_o^2) \frac{d}{d\mu} \left[ K_S^1(\mu_o) \right]^2} dS. \tag{D-8}$$

Taking account of the fact that  $K_S^1(\mu_o) = K_{-S}^1(\mu_o)$ , this can also be written in the form

$$- S_o = \frac{1 + \mu_o}{1 - \mu_o} - \frac{1}{\pi} \int_0^{\infty} \frac{S (4S^2 + 1) \sinh. (\pi S)}{(1 - \mu_o^2) \frac{d}{d\mu} \left[ K_S^1(\mu_o) \right]^2} dS. \tag{D-9}$$

From the relations  $(1 - \mu^2) \frac{dP_{\eta}^1}{d\mu} = \eta(\eta + 1) \sqrt{1 - \mu^2} P_{\eta} + \mu P_{\eta}^1$  and



$P_{\eta}^1 = -\sqrt{1-\mu^2} \frac{dP_{\eta}}{d\mu}$  it follows that

$$-S_o = \frac{1+\mu_o}{1-\mu_o} - \frac{1}{2\pi} \int_0^{\infty} \frac{S(4S^2+1) \sinh(\pi S) dS}{\frac{dK_S(\mu_o)}{d\mu} \left[ \mu_o \frac{dK_S(\mu_o)}{d\mu} + \left(S^2 + \frac{1}{4}\right) K_S(\mu_o) \right]} \quad (D-10)$$

From the expansion  $K_S(\cos \theta) = 1 + \frac{4\lambda^2 + 1^2}{2^2} \sin^2 \frac{\theta}{2}$

+  $\frac{(4\lambda^2 + 1^2)(4\lambda^2 + 3^2)}{2^2 4^2} \sin^4 \frac{\theta}{2} + \dots$  (Ref. 14, p. 74), it follows

that  $K_S$  is real for real  $S$  and  $\theta$ , and that  $K_S$  is a monotonic increasing function of  $S$ . From the reality of  $K_S$  it follows that the sum  $S$  is real. Another expression for  $K_S$  is

$$K_S(\cos \theta) = \frac{2}{\pi} \cosh(\pi S) \int_0^{\infty} \frac{\cos Su du}{\sqrt{2(\cos \theta + \cosh u)}} \quad (D-11)$$

From (D-11) it follows that  $K_o(\cos \theta) = \frac{2}{\pi} \cdot K\left(\sin \frac{\theta}{2}\right)$  where the right hand side of the last expression is the complete elliptic integral.

## APPENDIX E

LIST OF ERRORS OBSERVED IN UMM-87

Since the publication of UMM-87, several errors in that paper have been observed. These errors are as follows:

Equation (II-3) on page 5 of UMM-87 was taken from Reference 11, where Stratton used  $\hat{n}$  to denote the inwardly directed normal to the surface. Since  $\hat{n}$  denotes the outward normal in UMM-87,

- (1) the sign of Equation (II-3), p. 5, should be changed to +,
- (2) the sign of Equation (II-4), p. 6, should be changed to +,
- (3) the sign of Equation (II-5), p. 6, should be changed to +, and
- (4) the sentence at the bottom of p. 6 which reads "also Equation (55) on page 463 ....." should be deleted.

On page 35, a factor of 4 is missing in the right hand member of (A-7).

Equation (D-4) on page 47 contains a typographical error. The  $(1 - \mu)^2$  should be  $(1 - \mu^2)$ .

On pages 34 and 38 the statements about  $n_i$  not being an integer do not apply to  $n_i=0$  since  $\frac{dP_o(\mu)}{d\mu} = 0$ . In the vector case the term for  $n_i=0$  vanishes, but in the scalar case this term must be taken into account.

REFERENCES

1. R. C. Spencer, "Back Scattering From Conducting Surfaces", Air Force Cambridge Research Laboratories, CRL-E5070, April 1951.
2. W. W. Hansen, "Theoretical Study of Electromagnetic Waves From Shaped Metal Surfaces", Quarterly Report No. 1, Stanford University, Microwave Laboratory, ATI 133922, November 1947.
3. W. W. Hansen and L. I. Schiff, "Theoretical Study of Electromagnetic Waves Scattered From Shaped Metal Surfaces", Quarterly Report No. 2, Stanford University, Microwave Laboratory, ATI 133921, February 1948.
4. W. W. Hansen and L. I. Schiff, "Theoretical Study of Electromagnetic Waves Scattered From Shaped Metal Surfaces", Quarterly Report No. 3, Stanford University, Microwave Laboratory, ATI 104410, May 1948.
5. W. W. Hansen and L. I. Schiff, "Theoretical Study of Electromagnetic Waves Scattered From Shaped Metal Surfaces", Quarterly Report No. 4, Stanford University, Microwave Laboratory, ATI 46568, September 1948.
6. C. J. Sletten, "Electromagnetic Scattering From Wedges and Cones", Cambridge Research Center, Report CRC-E5090, July 1952.
7. P. M. Austin, Unpublished Research.
8. H. R. Alexander, "A Ripple Tank for Wave Propagation Studies", E. E. Department, Princeton University, PU-270-S/TR-5, TIP U16339, December 1950.
9. P. M. Morse, Vibration and Sound, McGraw-Hill Book Company, Inc., 1948.

REFERENCES (Continued)

10. L. I. Schiff, Quantum Mechanics, McGraw-Hill Book Company, Inc., 1949.
11. J. A. Stratton, Electromagnetic Theory, McGraw-Hill Book Company, Inc., 1941.
12. P. Debye, "Der Lichtdruck auf Kugeln von beliebigem Material", Annalen der Physik, p. 57, 30, Leipzig, 1909.
13. T. J. Bromwich, An Introduction to the Theory of Infinite Series, MacMillan and Co., 1947.
14. W. Magnus and F. Oberhettinger, Formulas and Theorems for the Special Functions of Mathematical Physics, Chelsea Publishing Co., 1949.
15. G. N. Watson, A Treatise on the Theory of Bessel Functions, 2nd Edition, Cambridge University Press, 1944.
16. S. A. Schelkunoff, Electromagnetic Waves, D. Van Nostrand Co., Inc., 1943.
17. K. M. Siegel, J. W. Crispin, R. E. Kleinman, H. E. Hunter, "The Zeros of  $P'_{n_i}(x_0)$  of Non-Integral Degree", Journal of Mathematics and Physics, Vol. 31, No. 3, pp. 170-179, October 1952.
18. K. M. Siegel, J. W. Crispin, R. E. Kleinman, H. E. Hunter, "Note on the Zeros of  $\frac{d P'_{m_i}(x)}{dx} \Big|_{x=x_0}$ ", to be published.
19. H. T. Davis, "Tables of the Higher Mathematical Functions",

REFERENCES (Continued)

Vol. I and II, the Principia Press, Inc., Bloomington, Indiana, 1933 and 1935.

20. K. M. Siegel, D. M. Brown, H. E. Hunter, H. A. Alperin, and C. W. Quillen, "The Zeros of the Associated Legendre Function  $P_n^m(\mu')$  of Non-Integral Degree", UMM-82, Willow Run Research Center, University of Michigan, April 1951.
21. H. M. MacDonald, "Zeros of the Spherical Harmonic  $P_n^m(\mu)$  Considered as a Function of  $n$ ", Proc. London Mathematical Society (1), Vol. XXXI, p. 264, 1899.

UMM-92

DISTRIBUTION

Distributed in accordance with  
the Terms of the Contract.



UNIVERSITY OF MICHIGAN



**3 9015 03525 0672**